Editors' Suggestion

Optical conductivity and damping of plasmons due to electron-electron interaction

Prachi Sharma,[1,2] Alessandro Principi,[3] Giovanni Vignale,[4] and Dmitrii L. Maslov[1,*]

[1]*Department of Physics, University of Florida, Gainesville, Florida 32611-8440, USA*

[2]*School of Physics and Astronomy, University of Minnesota, Minneapolis, Minnesota 55455, USA*

[3]*Department of Physics and Astronomy, University of Manchester, Oxford Road, M13 9PL Manchester, United Kingdom*

[4]*The Institute for Functional Intelligent Materials (I-FIM), National University of Singapore, 4 Science Drive 2, Singapore 117544*

(Received 7 October 2023; revised 18 December 2023; accepted 21 December 2023; published 24 January 2024)

We revisit the issue of plasmon damping due to electron-electron interaction. The plasmon linewidth can be related to the imaginary part of the charge susceptibility or, equivalently, to the real part of the optical conductivity, $\mathrm{Re}\sigma(q,\omega)$. Approaching the problem first via a standard semiclassical Boltzmann equation, we show that $\mathrm{Re}\sigma(q,\omega)$ of a two-dimensional (2D) electron gas scales as q^2T^2/ω^4 for $\omega \ll T$, which agrees with the results of Principi *et al.* [Phys. Rev. B **88**, 195405 (2013)] and Sharma *et al.* [Phys. Rev. B **104**, 045142 (2021)] but disagrees with that of Mishchenko *et al.* [Phys. Rev. B **69**, 195302 (2004)], according to which $\mathrm{Re}\sigma(q,\omega) \propto q^2T^2/\omega^2$. To resolve this disagreement, we rederive $\mathrm{Re}\sigma(q,\omega)$ using the original method of Mishchenko *et al.* for an arbitrary ratio ω/T and show that while the last term is, indeed, present, it is subleading to the q^2T^2/ω^4 term. We give a physical interpretation of both leading and subleading contributions in terms of the shear and bulk viscosities of an electron liquid, respectively. We also calculate $\mathrm{Re}\sigma(q,\omega)$ for a three-dimensional electron gas and doped monolayer graphene. We find that, all other parameters being equal, finite temperature has the strongest effect on the plasmon linewidth in graphene, where it scales as $T^4 \ln T$ for $\omega \ll T$.

DOI: 10.1103/PhysRevB.109.045431

I. INTRODUCTION

Collective modes of a Fermi liquid (FL) are the direct manifestation of its many-body nature. In a charged FL, the most well-studied mode is the plasmon. The plasmon dispersion and linewidth contain important information about the many-body dynamics in electron systems and are also crucial parameters for plasmonic devices. Traditionally, plasmons have been observed by electron energy-loss spectroscopy [1]. The interest in plasmon dynamics has recently intensified due to near-field optical spectroscopy of graphene-based devices [2–4] and momentum-resolved electron energy-loss spectroscopy of superconducting cuprates and related compounds [5]. On the theoretical side, within the random-phase approximation (RPA) and at $T = 0$ a plasmon has an infinitely long lifetime as long as it stays outside the particle-hole continuum and thus cannot decay via the Landau-damping mechanism [6]. Beyond the RPA, plasmons do decay into multiple particle-hole pairs. In terms of Feynman diagrams, these processes are accounted for by dressing the free particle-hole bubbles with interaction lines. Damping of plasmons in three dimensions (3D) was studied by DuBois and Kivelson as early as in 1969 [7]. Damping of plasmons in two dimensions (2D) was studied in Refs. [8–14] in both the collisionless and hydrodynamic regimes. However, the results of different papers for damping in the collisionless regime [8–11,14] do not always agree with each other, although all of them are obtained under the same assumptions, the most important of which is weak coupling. The goal of this communication is to finalize the result for the lifetime of plasmons due to electron-electron interaction, at least at weak coupling. We will limit our attention to the collisionless regime, which occurs if the plasmon frequency is much higher than the rate of relaxation towards equilibrium, and consider the cases of 2D and 3D electron gases with parabolic dispersion, as well as of doped monolayer graphene. We will also consider only damping due to intraband excitations, although interband excitations need to be accounted for to explain plasmon damping in real materials [15]. In what follows, we set $k_B = 1$ and $\hbar = 1$.

Formally, damping of plasmons is due to the fact that the imaginary part of the charge susceptibility $\chi_c(q,\omega)$ is finite outside the particle-hole continuum. Thanks to the Einstein relation [16,17]

$$\mathrm{Re}\sigma(q,\omega) = \frac{e^2\omega}{q^2}\mathrm{Im}\chi_c(q,\omega), \tag{1}$$

the same condition can be reformulated in terms of the real part of the conductivity. To facilitate the comparison, we list below the results of different papers for $\mathrm{Re}\sigma(q,\omega)$ [18].

Mishchenko, Reizer, and Glazman (MRG) [10] considered a Galilean-invariant 2D electron gas (2DEG), i.e., a 2D electron system with $\epsilon_{\mathbf{k}} = k^2/2m$ dispersion. Using an original

*maslov@ufl.edu

Published by the American Physical Society under the terms of the Creative Commons Attribution 4.0 International license. Further distribution of this work must maintain attribution to the author(s) and the published article's title, journal citation, and DOI.

method to calculate the absorption rate of electromagnetic radiation by electrons, they obtained the following result for the conductivity at finite q, ω, and T:

$$\mathrm{Re}\sigma(q,\omega) = \frac{e^2}{12\pi^2}\frac{q^2}{k_\mathrm{F}^2}\frac{\omega^2+4\pi^2T^2}{\omega^2}\ln\frac{v_\mathrm{F}\kappa}{\max\{|\omega|,T\}}, \quad (2)$$

where k_F and v_F are the Fermi momentum and velocity, respectively, and $\kappa = 2me^2$ is the inverse radius of the screened Coulomb interaction in 2D, defined by

$$V_\mathbf{Q} = \frac{2\pi e^2}{Q+\kappa}. \quad (3)$$

Equation (2) is derived under the following assumptions: $\max\{\omega,T\} \ll v_\mathrm{F}\kappa \lesssim E_\mathrm{F}$ and $q \ll \max\{\omega,T\}/v_\mathrm{F}$. (We remind the reader that $v_\mathrm{F}\kappa \ll E_\mathrm{F}$ at weak coupling.) The results of this paper will also be obtained under the same assumptions. Please note that henceforth T stands for the temperature of the electron system, which may be different from the lattice temperature; for example, Ref. [3] reports the electron temperature of graphene under near-field pumping to be as high as 3200 K.

The vanishing of $\mathrm{Re}\sigma(q,\omega)$ in Eq. (2) at $q=0$ reflects the fact that internal forces in a Galilean-invariant system do not affect the motion of the center of mass and, therefore, the dissipative part of the conductivity must vanish at $q=0$ and finite ω. Such a constraint is no longer valid for graphene, which is not a Galilean-invariant system. Indeed, the low-energy excitations near the K and K' points of the Brillouin zone in graphene have a linear (Dirac) dispersion. This in turn implies that the velocity is constant in magnitude and given by $\boldsymbol{v}_\boldsymbol{k} = v_\mathrm{D}\hat{\boldsymbol{k}}$. Therefore, momentum conservation does not automatically imply current conservation, as it does in Galilean-invariant systems. As a result, graphene has a finite optical conductivity even in the presence of a uniform *ac* field, i.e., at $q=0$. The optical conductivity of graphene away from the charge neutrality was analyzed in Refs. [8,9], which identified the limiting form of the conductivity at $q=0$. In addition, Refs. [8,9] presented an $O(q^2)$ term, which is necessary for determining the plasmon linewidth. The complete result, as derived in Ref. [9], reads

$$\mathrm{Re}\sigma(q,\omega) = \mathrm{Re}\sigma_1(\omega) + \mathrm{Re}\sigma_2(q,\omega), \quad (4a)$$

$$\mathrm{Re}\sigma_1(\omega) = \frac{e^2}{240}\frac{\omega^2}{E_\mathrm{F}^2}\left(1+4\pi^2\frac{T^2}{\omega^2}\right) \times\left(3+8\pi^2\frac{T^2}{\omega^2}\right)\ln\frac{v_\mathrm{D}\kappa}{\max\{|\omega|,2\pi T\}}, \quad (4b)$$

$$\mathrm{Re}\sigma_2(q,\omega) = \frac{e^2}{24\pi^2}\frac{q^2\kappa^2}{m^{*2}\omega^2}\left(1+4\pi^2\frac{T^2}{\omega^2}\right)\ln\frac{k_\mathrm{F}}{\kappa}, \quad (4c)$$

where $\mathrm{Re}\sigma_1(\omega)$ and $\mathrm{Re}\sigma_2(q,\omega)$ are the $O(q^0)$ and $O(q^2)$ contributions, respectively, v_D is the Dirac velocity, which plays the role of v_F for the Dirac spectrum, and $m^* = k_\mathrm{F}/v_\mathrm{D}$ [19]. Note that although $\mathrm{Re}\sigma_1$ is finite at $q=0$, it is suppressed by a factor of $(\omega/E_\mathrm{F})^2$ compared with a regular FL contribution [20,21].

It was further conjectured in Refs. [8,9] that the $O(q^2)$ contribution should be the same for the Dirac and parabolic spectra, up to the redefinitions of the effective mass and inverse screening length, i.e., the optical conductivity of a 2DEG should read

$$\mathrm{Re}\sigma(q,\omega) = \frac{e^2}{24\pi^2}\frac{q^2\kappa^2}{m^2\omega^2}\left(1+4\pi^2\frac{T^2}{\omega^2}\right)\ln\frac{k_\mathrm{F}}{\kappa}. \quad (5)$$

If this is the case (and we will show explicitly that it is), then there is a contradiction with the MRG result, Eq. (2). Indeed, Eqs. (2) and (5) differ by a factor of $(v_\mathrm{F}\kappa/\omega)^2 \sim \omega_\mathrm{p}^2(\kappa)/\omega^2$, where $\omega_\mathrm{p}(q)$ is the plasmon dispersion. This implies that Eq. (5) is parametrically larger than Eq. (2) for $\omega \ll \omega_\mathrm{p}(\kappa)$.

The difference between Eqs. (2) and (5) is not purely mathematical. In fact, the corresponding contributions arise from different physical processes and, on a general level, are related to the bulk and shear viscosities of the electron liquid, correspondingly.

The real part of the optical conductivity is related to the plasmon linewidth, $\Gamma(q)$, defined by the complex dispersion relation $\omega = \omega_\mathrm{p}(q) - i\Gamma(q)$. In 2D [10],

$$\Gamma(q) = \pi q\,\mathrm{Re}\sigma(q,\omega)|_{\omega=\omega_\mathrm{p}(q)}. \quad (6)$$

In a 2DEG, $\omega_\mathrm{p}(q) = v_\mathrm{F}\sqrt{\kappa q/2}$. Accordingly, Eqs. (2) and (4c) give quite different results for the plasmon linewidth. At $T=0$, for example,

$$\Gamma(q)|_{\text{Eq. (2)}}/\Gamma(q)|_{\text{Eq. (4c)}} \sim q/\kappa, \quad (7)$$

which is smaller than unity for $q \ll \kappa$.

The approaches employed in previous works [8–10] involve quite complicated computations. We find it instructive to start with a more straightforward approach, namely, with a semiclassical Boltzmann equation, which is valid for $\omega \ll T$. In this regime, Eqs. (2) and (5) reduce to

$$\mathrm{Re}\sigma(q,\omega) = \frac{e^2}{3k_\mathrm{F}^2}\frac{q^2T^2}{\omega^2}\ln\frac{v_\mathrm{F}\kappa}{T} \quad (8)$$

and

$$\mathrm{Re}\sigma(q,\omega) = \frac{e^2\kappa^2}{6m^2}\frac{q^2T^2}{\omega^4}\ln\frac{k_\mathrm{F}}{\kappa}, \quad (9)$$

respectively, and it should be fairly easy to see which one is correct. This exercise is the subject of Sec. II.

The rest of this paper is organized as follows. Section III A gives a brief review of the MRG method. In Sec. III B, we rederive the result for the optical conductivity of a 2DEG using the MRG method and show that, in agreement with the conjectures of Refs. [8,9], it is given by Eq. (5) rather than Eq. (2). We must emphasize that the error in Ref. [10] is purely computational and reflects neither on the MRG method itself nor on the results of this reference for plasmon damping due to electron-phonon interaction. Using the MRG method, we also calculate the optical conductivity of a 3D electron gas in Sec. III C and supply the details of the derivation of Eqs. (4a)–(4c) for graphene. In Sec. IV, we give a physical interpretation of our results in terms of the bulk and shear viscosities of an electron liquid. In Sec. V, we discuss the plasmon linewidth. Section VI presents our conclusions.

II. OPTICAL CONDUCTIVITY VIA THE SEMICLASSICAL BOLTZMANN EQUATION

In this section, we calculate the longitudinal conductivity of a 2D Galilean-invariant electron system, using the semiclassical Boltzmann equation (BE) with a collision integral that does not depend on the frequency of an external electric field. Such a BE is valid for $\omega \ll T$. Assuming the electric field to be of the form $\mathbf{E} = \mathbf{E}_0 e^{i(\mathbf{q}\cdot\mathbf{r}-\omega t)}$, the BE for the Fourier transform of the nonequilibrium part of the distribution function $\delta f(\mathbf{q},\omega;\mathbf{k}) \equiv \delta f_{\mathbf{k}}$ reads

$$-i(\omega - \mathbf{v}_{\mathbf{k}}\cdot\mathbf{q} + i0^+)\delta f_{\mathbf{k}} - e(\mathbf{E}_0\cdot\mathbf{v}_{\mathbf{k}})n'_{\mathbf{k}} = I_{\mathrm{ee}}[\delta f_{\mathbf{k}}], \quad (10)$$

where $n_{\mathbf{k}} = n_{\mathrm{F}}(\varepsilon_{\mathbf{k}})$ is the Fermi function, $n'_{\mathbf{k}} = \partial n_{\mathrm{F}}(\varepsilon_{\mathbf{k}})/\partial\varepsilon_{\mathbf{k}}$, $I_{\mathrm{ee}}[\delta f_{\mathbf{k}}]$ is the electron-electron collision integral, and an infinitesimally small imaginary term $i0^+$ was added to ensure the retarded nature of the response. With a definition $\delta f_{\mathbf{k}} = n_{\mathbf{k}}(1-n_{\mathbf{k}})g_{\mathbf{k}} = -Tn'_{\mathbf{k}}g_{\mathbf{k}}$, the equation for $g_{\mathbf{k}}$ reads [22]

$$i(\omega - \mathbf{v}_{\mathbf{k}}\cdot\mathbf{q} + i0^+)g_{\mathbf{k}} - \frac{e}{T}(\mathbf{E}_0\cdot\mathbf{v}_{\mathbf{k}}) = \frac{1}{Tn'_{\mathbf{k}}}\int_{\mathbf{k}'\mathbf{p}\mathbf{p}'} W_{\mathbf{k},\mathbf{p}\to\mathbf{k}'\mathbf{p}'}(1-n_{\mathbf{k}'})(1-n_{\mathbf{p}'})n_{\mathbf{p}}n_{\mathbf{k}}\delta(\varepsilon_{\mathbf{k}}+\varepsilon_{\mathbf{p}}-\varepsilon_{\mathbf{k}'}-\varepsilon_{\mathbf{p}'})$$
$$\times\,\delta(\mathbf{k}+\mathbf{p}-\mathbf{k}'-\mathbf{p}')(g_{\mathbf{k}}+g_{\mathbf{p}}-g_{\mathbf{k}'}-g_{\mathbf{p}'}), \quad (11)$$

where $W_{\mathbf{k},\mathbf{p}\to\mathbf{k}'\mathbf{p}'}$ is the scattering probability and $\int_{\mathbf{k}}$ is a shorthand for $\int d^2k/(2\pi)^2$ (and similarly for other momenta). The overall scale of the collision integral is given by the relaxation rate due to electron-electron interactions at finite T, $1/\tau_{\mathrm{ee}}(T)$. The temperature is assumed to be low enough so that the condition $1/\tau_{\mathrm{ee}}(T) \ll \omega$ is satisfied (yet high enough such that $T \gg \omega$). In this case, Eq. (11) can be solved by subsequent iterations in the collision integral. To zeroth order, we neglect the collision integral and obtain

$$g^{(0)}_{\mathbf{k}} = \frac{1}{T}\frac{e(\mathbf{E}_0\cdot\mathbf{v}_{\mathbf{k}})}{i(\omega - \mathbf{v}_{\mathbf{k}}\cdot\mathbf{q} + i0^+)}. \quad (12)$$

At the next step, we substitute $g_{\mathbf{k}} = g^{(0)}_{\mathbf{k}} + g^{(1)}_{\mathbf{k}}$ back into Eq. (11) and neglect $g^{(1)}_{\mathbf{k}}$ inside the collision integral, to obtain

$$g^{(1)}_{\mathbf{k}} = \frac{e}{n'_{\mathbf{k}}T^2(\omega - \mathbf{v}_{\mathbf{k}}\cdot\mathbf{q} + i0^+)}\int_{\mathbf{k}'\mathbf{p}\mathbf{p}'} W_{\mathbf{k},\mathbf{p}\to\mathbf{k}'\mathbf{p}'}(1-n_{\mathbf{k}'})(1-n_{\mathbf{p}'})n_{\mathbf{p}}n_{\mathbf{k}}\delta(\varepsilon_{\mathbf{k}}+\varepsilon_{\mathbf{p}}-\varepsilon_{\mathbf{k}'}-\varepsilon_{\mathbf{p}'})$$
$$\times\,\delta(\mathbf{k}+\mathbf{p}-\mathbf{k}'-\mathbf{p}')\left(\frac{\mathbf{v}_{\mathbf{k}}}{\omega-\mathbf{v}_{\mathbf{k}}\cdot\mathbf{q}} + \frac{\mathbf{v}_{\mathbf{p}}}{\omega-\mathbf{v}_{\mathbf{p}}\cdot\mathbf{q}} - \frac{\mathbf{v}_{\mathbf{k}'}}{\omega-\mathbf{v}_{\mathbf{k}'}\cdot\mathbf{q}} - \frac{\mathbf{v}_{\mathbf{p}'}}{\omega-\mathbf{v}_{\mathbf{p}'}\cdot\mathbf{q}}\right)\cdot\mathbf{E}_0. \quad (13)$$

The conductivity is read off from the electrical current $\mathbf{j} = -e\int_{\mathbf{k}}\delta f_{\mathbf{k}}\mathbf{v}_{\mathbf{k}} = Te\int_{\mathbf{k}} n'_{\mathbf{k}}g_{\mathbf{k}}\mathbf{v}_{\mathbf{k}}$, as a coefficient of linear proportionality between $\mathbf{j}$ and $\mathbf{E}$. As we are interested in the longitudinal part of the conductivity, we choose $\mathbf{q} \parallel \mathbf{E}$. Then the conductivity can be found as

$$\mathrm{Re}\sigma(q,\omega) = \tfrac{1}{2}[\mathrm{Re}\sigma_{xx}(q,\omega) + \mathrm{Re}\sigma_{yy}(q,\omega)], \quad (14)$$

where $\sigma_{\alpha\alpha}(q,\omega)$ denotes the conductivity calculated with both $\mathbf{E}$ and $\mathbf{q}$ being along the α axis.

The real part of the zeroth-order conductivity, obtained from Eq. (12), is nonzero only within the particle-hole continuum, i.e., for $|\omega| < v_{\mathrm{F}}q$, and is not relevant here, while the first-order correction in Eq. (13) yields

$$\mathrm{Re}\sigma(q,\omega) = \frac{e^2}{8T}\int_{\mathbf{k}\mathbf{p}\mathbf{k}'\mathbf{p}'} W_{\mathbf{k},\mathbf{p}\to\mathbf{k}'\mathbf{p}'}(1-n_{\mathbf{k}'})(1-n_{\mathbf{p}'})n_{\mathbf{p}}n_{\mathbf{k}}\delta(\varepsilon_{\mathbf{k}}+\varepsilon_{\mathbf{p}}-\varepsilon_{\mathbf{k}'}-\varepsilon_{\mathbf{p}'})\delta(\mathbf{k}+\mathbf{p}-\mathbf{k}'-\mathbf{p}')$$
$$\times\left(\frac{\mathbf{v}_{\mathbf{k}}}{\omega-\mathbf{v}_{\mathbf{k}}\cdot\mathbf{q}} + \frac{\mathbf{v}_{\mathbf{p}}}{\omega-\mathbf{v}_{\mathbf{p}}\cdot\mathbf{q}} - \frac{\mathbf{v}_{\mathbf{k}'}}{\omega-\mathbf{v}_{\mathbf{k}'}\cdot\mathbf{q}} - \frac{\mathbf{v}_{\mathbf{p}'}}{\omega-\mathbf{v}_{\mathbf{p}'}\cdot\mathbf{q}}\right)^2. \quad (15)$$

To arrive at the last result, we used the symmetry properties of $W_{\mathbf{k},\mathbf{p}\to\mathbf{k}'\mathbf{p}'}$ [23,24]. At $\mathbf{q} = 0$, the second line of Eq. (15) is reduced to $(\mathbf{v}_{\mathbf{k}} + \mathbf{v}_{\mathbf{p}} - \mathbf{v}_{\mathbf{k}'} - \mathbf{v}_{\mathbf{p}'})^2/\omega^2$, which vanishes identically for the Galilean-invariant case, when $\mathbf{v}_{\mathbf{k}} = \mathbf{k}/m$. A finite result for the conductivity is obtained by expanding Eq. (15) in q. To order q^2, we obtain

$$\mathrm{Re}\sigma(q,\omega) = \frac{e^2q^2}{8T\omega^4}\int_{\mathbf{k}\mathbf{p}\mathbf{k}'\mathbf{p}'} W_{\mathbf{k},\mathbf{p}\to\mathbf{k}'\mathbf{p}'}(1-n_{\mathbf{k}'})(1-n_{\mathbf{p}'})n_{\mathbf{p}}n_{\mathbf{k}}\delta(\varepsilon_{\mathbf{k}}+\varepsilon_{\mathbf{p}}-\varepsilon_{\mathbf{k}'}-\varepsilon_{\mathbf{p}'})\delta(\mathbf{k}+\mathbf{p}-\mathbf{k}'-\mathbf{p}')$$
$$\times[\mathbf{v}_{\mathbf{k}}(\mathbf{v}_{\mathbf{k}}\cdot\hat{\mathbf{q}}) + \mathbf{v}_{\mathbf{p}}(\mathbf{v}_{\mathbf{p}}\cdot\hat{\mathbf{q}}) - \mathbf{v}_{\mathbf{k}'}(\mathbf{v}_{\mathbf{k}'}\cdot\hat{\mathbf{q}}) - \mathbf{v}_{\mathbf{p}'}(\mathbf{v}_{\mathbf{p}'}\cdot\hat{\mathbf{q}})]^2, \quad (16)$$

where $\hat{\mathbf{q}} = \mathbf{q}/q$. The general form of $\mathrm{Re}\sigma(q,\omega)$ can be deduced already at this step. Indeed, Eq. (16) contains integrals over three independent energies (say, $\varepsilon_{\mathbf{k}}$, $\varepsilon_{\mathbf{p}}$, and $\varepsilon_{\mathbf{k}'}$), each of them contributing a factor of T to the final result. Therefore

$$\mathrm{Re}\sigma(q,\omega) \propto \frac{q^2T^2}{\omega^4}, \quad (17)$$

which is consistent with Eq. (9).

The result (17) can be understood in the following way. A factor of q^2 follows immediately from the fact that $\mathrm{Re}\sigma(q,\omega)$ must vanish at $q=0$ and be analytic in q (at finite ω and T). The scaling $1/\omega^4$ follows from the fact that we need to iterate the BE once and expand the result in $v_{\mathrm{F}}q/\omega$. Finally, the factor of T^2 is the expected FL scaling of the scattering rate.

The rest of the calculation proceeds assuming that $W_{\mathbf{k},\mathbf{p}\to\mathbf{k}'\mathbf{p}'}$ is given by the Born approximation for the screened Coulomb potential (3), i.e., $W_{\mathbf{k},\mathbf{p}\to\mathbf{k}'\mathbf{p}'}=8\pi V^2_{\mathbf{k}-\mathbf{k}'}$. After a straightforward calculation (see Appendix B), we arrive at

$$\mathrm{Re}\sigma(q,\omega)=\frac{e^2\kappa^2}{6m^2}\frac{q^2T^2}{\omega^4}\ln\frac{k_{\mathrm{F}}}{\kappa}, \tag{18}$$

which coincides with Eq. (9) rather than with Eq. (8). Given also that the conductivity must satisfy the first-Matsubara-frequency rule [25–27], i.e., $\sigma(\omega=\pm 2\pi iT,T)=0$, one can generalize the result in Eq. (18) for the case of an arbitrary ratio of ω to T as $\mathrm{Re}\sigma(q,\omega)\propto q^2(\omega^2+4\pi^2T^2)/\omega^4$, which is Eq. (5). In the next section, we will see that this is, indeed, the correct result.

III. OPTICAL CONDUCTIVITY VIA THE MISHCHENKO-REIZER-GLAZMAN METHOD

In this section, we resolve the disagreement between the result of Ref. [10] and the results of Refs. [8,9] and finalize the correct expression for the optical conductivity of a 2DEG. Using the MRG method, we will show that in addition to the contribution found by MRG [Eq. (2)], there is also another contribution given by Eq. (5). For completeness, we will also derive the expressions for the optical conductivities of a 3D electron gas and graphene in Secs. III C and III D, respectively.

A. MRG method

In the MRG method, one calculates the rate at which electromagnetic radiation is absorbed by a system of interacting electrons. The differential probability of an electron-electron collision in the presence of a photon is written via the Fermi golden rule as

$$dw_{s,s_z}=2\pi|\mathcal{L}_{s,s_z}|^2\delta(\varepsilon_{\mathbf{p}}+\varepsilon_{\mathbf{k}}-\varepsilon_{\mathbf{p}'}-\varepsilon_{\mathbf{k}'}+\omega)\times\delta(\mathbf{p}+\mathbf{k}-\mathbf{k}'-\mathbf{p}'+\mathbf{q})\frac{d^Dp'd^Dk'}{(2\pi)^2}, \tag{19}$$

where $\mathbf{p}$, $\mathbf{k}$ ($\mathbf{p}'$, $\mathbf{k}'$) are the initial (final) momenta of electrons, s is the total spin of two electrons in the initial state, s_z is the spin projection on the quantization axis, and $\mathcal{L}_{s,s_z}$ is the matrix element which depends on s and, in general, on s_z. To first order in the screened Coulomb interaction, the matrix elements for the singlet and triplet states are given by

$$\mathcal{L}_{0,0}=e\phi_0\left(\frac{V_{\mathbf{k}-\mathbf{k}'}+V_{\mathbf{p}'-\mathbf{k}}}{\varepsilon_{\mathbf{p}}-\varepsilon_{\mathbf{p}+\mathbf{q}}+\omega}+\frac{V_{\mathbf{k}-\mathbf{k}'}+V_{\mathbf{p}-\mathbf{k}'}}{\varepsilon_{\mathbf{p}'}-\varepsilon_{\mathbf{p}'-\mathbf{q}}-\omega}+\frac{V_{\mathbf{p}'-\mathbf{p}}+V_{\mathbf{p}-\mathbf{k}'}}{\varepsilon_{\mathbf{k}}-\varepsilon_{\mathbf{k}+\mathbf{q}}+\omega}+\frac{V_{\mathbf{p}'-\mathbf{p}}+V_{\mathbf{p}'-\mathbf{k}}}{\varepsilon_{\mathbf{k}'}-\varepsilon_{\mathbf{k}'-\mathbf{q}}-\omega}\right) \tag{20}$$

and

$$\mathcal{L}_{1,0}=\mathcal{L}_{1,\pm1}=e\phi_0\left(\frac{V_{\mathbf{k}-\mathbf{k}'}-V_{\mathbf{p}'-\mathbf{k}}}{\varepsilon_{\mathbf{p}}-\varepsilon_{\mathbf{p}+\mathbf{q}}+\omega}+\frac{V_{\mathbf{k}-\mathbf{k}'}-V_{\mathbf{p}-\mathbf{k}'}}{\varepsilon_{\mathbf{p}'}-\varepsilon_{\mathbf{p}'-\mathbf{q}}-\omega}+\frac{V_{\mathbf{p}'-\mathbf{p}}-V_{\mathbf{p}-\mathbf{k}'}}{\varepsilon_{\mathbf{k}}-\varepsilon_{\mathbf{k}+\mathbf{q}}+\omega}+\frac{V_{\mathbf{p}'-\mathbf{p}}-V_{\mathbf{p}'-\mathbf{k}}}{\varepsilon_{\mathbf{k}'}-\varepsilon_{\mathbf{k}'-\mathbf{q}}-\omega}\right), \tag{21}$$

respectively, where $q\phi_0$ is the in-plane component of the electric field of an electromagnetic wave.

Next, one derives the total probability of absorption using Eq. (19) with matrix elements from Eq. (20), which is then used to calculate the dissipation rate. The latter is then related to the real part of the longitudinal conductivity, which is given by [10]

$$\mathrm{Re}\sigma(q,\omega)=\frac{(1-e^{-\omega/T})}{4q^2\omega^3\phi_0^2}\iiiint\frac{d^Dpd^Dkd^Dp'd^Dk'}{(2\pi)^{3D-1}}(|\mathcal{L}_{0,0}|^2+3|\mathcal{L}_{1,0}|^2)n_{\mathbf{k}}n_{\mathbf{p}}(1-n_{\mathbf{p}'})(1-n_{\mathbf{k}'})\times\delta(\varepsilon_{\mathbf{p}}+\varepsilon_{\mathbf{k}}-\varepsilon_{\mathbf{p}'}-\varepsilon_{\mathbf{k}'}+\omega)\delta(\mathbf{p}+\mathbf{k}-\mathbf{k}'-\mathbf{p}'+\mathbf{q}). \tag{22}$$

The matrix elements can be written as $\mathcal{L}_{0,0}=e\phi_0(\mathcal{A}+\mathcal{A}_{\mathrm{ex}})/\omega^2$ and $\mathcal{L}_{1,0}=e\phi_0(\mathcal{A}-\mathcal{A}_{\mathrm{ex}})/\omega^2$, where

$$\mathcal{A}=\omega^2\left[V_{\mathbf{k}-\mathbf{k}'}\left(\frac{1}{\varepsilon_{\mathbf{p}}-\varepsilon_{\mathbf{p}+\mathbf{q}}+\omega}+\frac{1}{\varepsilon_{\mathbf{p}'}-\varepsilon_{\mathbf{p}'-\mathbf{q}}-\omega}\right)+V_{\mathbf{p}'-\mathbf{p}}\left(\frac{1}{\varepsilon_{\mathbf{k}}-\varepsilon_{\mathbf{k}+\mathbf{q}}+\omega}+\frac{1}{\varepsilon_{\mathbf{k}'}-\varepsilon_{\mathbf{k}'-\mathbf{q}}-\omega}\right)\right] \tag{23}$$

and $\mathcal{A}_{\mathrm{ex}}$ is the exchange term obtained by interchanging $\mathbf{p}'\leftrightarrow\mathbf{k}'$ in Eq. (23) [28]. From now on, we will neglect the exchange term $\mathcal{A}_{\mathrm{ex}}$, which contains the interaction potential at large momenta transfers and is, therefore, small for a weakly screened Coulomb interaction. It is also convenient to introduce the momentum and energy transfers via $\mathbf{Q}=\mathbf{p}-\mathbf{p}'=\mathbf{k}'-\mathbf{k}-\mathbf{q}$ and $\Omega=\varepsilon_{\mathbf{p}}-\varepsilon_{\mathbf{p}'}=\varepsilon_{\mathbf{k}'}-\varepsilon_{\mathbf{k}}-\omega$, respectively, upon which Eq. (22) becomes

$$\mathrm{Re}\sigma(q,\omega)=\frac{e^2(1-e^{-\omega/T})}{(2\pi)^{3D-1}q^2\omega^3}\iiiint d^DQd^Dpd^Dkd\Omega\,\mathcal{A}^2\,n_{\mathrm{F}}(\varepsilon_{\mathbf{k}})n_{\mathrm{F}}(\varepsilon_{\mathbf{p}})[1-n_{\mathrm{F}}(\varepsilon_{\mathbf{p}}-\Omega)][1-n_{\mathrm{F}}(\varepsilon_{\mathbf{k}}+\Omega+\omega)]\times\delta(\varepsilon_{\mathbf{p}}-\varepsilon_{\mathbf{p}-\mathbf{Q}}-\Omega)\delta(\varepsilon_{\mathbf{k}}-\varepsilon_{\mathbf{k}+\mathbf{Q}+\mathbf{q}}+\Omega+\omega). \tag{24}$$

Interestingly, the last formula can be expressed as a convolution of two free-electron response functions. For example, as shown in Appendix D, the dominant contribution to the conductivity of a Galilean-invariant system can be cast in the following form:

$$\mathrm{Re}\sigma(q,\omega) = b_D \frac{e^2 q^2}{\omega^5 m^2} \int \frac{d^D Q Q^2}{(2\pi)^D} \int_{-\infty}^{\infty} \frac{d\Omega}{\pi} V_{\mathbf{Q}}^2 [n_{\mathrm{B}}(\Omega) - n_{\mathrm{B}}(\Omega-\omega)] \mathrm{Im}\chi_T(Q,\Omega-\omega)\mathrm{Im}\chi_c(Q,\Omega), \tag{25}$$

where $n_{\mathrm{B}}(z)$ is the Bose function, $b_D = 8/15$ for $D = 3$ and $b_D = 1/2$ for $D = 2$, and where we have introduced the imaginary parts of the density-density response function [17]

$$\mathrm{Im}\chi_c(Q,\nu) \equiv -2\pi \int \frac{d^D k}{(2\pi)^D} [n_{\mathrm{F}}(\varepsilon_{\mathbf{k}-\mathbf{Q}/2}) - n_{\mathrm{F}}(\varepsilon_{\mathbf{k}+\mathbf{Q}/2})] \delta(\mathbf{k}\cdot\mathbf{Q}/m - \nu) \tag{26}$$

and of the transverse current-current response function

$$\mathrm{Im}\chi_T(Q,\nu) \equiv -2\pi \int \frac{d^D k}{(2\pi)^D} [n_{\mathrm{F}}(\varepsilon_{\mathbf{k}-\mathbf{Q}/2}) - n_{\mathrm{F}}(\varepsilon_{\mathbf{k}+\mathbf{Q}/2})] |\mathbf{k}\times\hat{\mathbf{Q}}/m|^2 \delta(\mathbf{k}\cdot\mathbf{Q}/m - \nu). \tag{27}$$

(The factors of 2 in the equations above account for spin degeneracy.) In the zero-temperature limit, the Ω integral is restricted to the range $0 < \Omega < \omega$ (for positive ω). Furthermore, because both response functions vanish linearly at low frequency, we see that the integral goes as ω^3, and the final result for the conductivity is proportional to q^2/ω^2, as it should. Similar formulas for the subdominant contributions to the conductivity of Galilean-invariant systems are provided in Appendix D. Equation (25) helps to elucidate the nature of excitations responsible for plasmon damping, as will be discussed in detail in Sec. IV.

We now proceed with applying Eq. (24) to specific cases.

B. Two-dimensional electron gas

First, we consider a 2D electron gas with a parabolic dispersion $\varepsilon_{\mathbf{k}} = k^2/2m$. As we are interested in the limit of $v_{\mathrm{F}} q/\omega \ll 1$, we expand $\mathcal{A}$ in Eq. (23) in $1/\omega$ as

$$\mathcal{A} = \mathcal{A}_1 + \mathcal{A}_2, \tag{28a}$$

$$\mathcal{A}_1 = V_{\mathbf{k}-\mathbf{k}'}\left[(\mathbf{v}_{\mathbf{p}} - \mathbf{v}_{\mathbf{p}'})\cdot\mathbf{q} + \frac{q^2}{m}\right] + V_{\mathbf{p}-\mathbf{p}'}\left[(\mathbf{v}_{\mathbf{k}} - \mathbf{v}_{\mathbf{k}'})\cdot\mathbf{q} + \frac{q^2}{m}\right], \tag{28b}$$

$$\mathcal{A}_2 = \frac{1}{\omega}\{V_{\mathbf{k}-\mathbf{k}'}[(\mathbf{v}_{\mathbf{p}}\cdot\mathbf{q})^2 - (\mathbf{v}_{\mathbf{p}'}\cdot\mathbf{q})^2] + V_{\mathbf{p}-\mathbf{p}'}[(\mathbf{v}_{\mathbf{k}}\cdot\mathbf{q})^2 - (\mathbf{v}_{\mathbf{k}'}\cdot\mathbf{q})^2]\}. \tag{28c}$$

The $\mathcal{A}_1$ term in the equation above is the one that was found in Ref. [10]. However, as will be shown below, one also needs to keep the $\mathcal{A}_2$ term, despite the fact that it appears to be next order in $1/\omega$. [Note that we have already neglected $O(q^4)$ terms in $\mathcal{A}_2$.]

Expanding the interaction potential as $V_{\mathbf{Q}+\mathbf{q}} = V_{\mathbf{Q}} + \mathbf{q}\cdot\nabla_{\mathbf{Q}} V_{\mathbf{Q}}$ and retaining only up to $O(q^2)$ terms, we rewrite $\mathcal{A}_1$ in Eq. (28b) as

$$\mathcal{A}_1 = \frac{1}{m}[q^2 V_{\mathbf{Q}} + (\mathbf{Q}\cdot\mathbf{q})(\mathbf{q}\cdot\nabla V_{\mathbf{Q}})]. \tag{29}$$

The MRG result, Eq. (2), is reproduced by keeping the first term in the equation above. Indeed, each of the three energy integrations in Eq. (24) (over $\varepsilon_{\mathbf{k}}$, $\varepsilon_{\mathbf{p}}$, and Ω) contribute a factor of ω, thereby canceling out a factor of $1/\omega^3$. Next, each of the two delta functions contributes a factor of $1/Q$, which leads to a logarithmic divergence in the integral over Q at the lower limit. Cutting off this divergence at $Q \sim \omega/v_{\mathrm{F}}$, we reproduce the structure of Eq. (2). Since the second term in Eq. (29) contains an extra factor of Q, the resultant Q integration does not lead to a logarithmic divergence and is thus subleading in the leading-logarithm sense.

Now, we turn to the "new" (compared with MRG) term, $\mathcal{A}_2$ in Eq. (28c). Expanding this term to order q^2, we obtain

$$\mathcal{A}_2 = \frac{2V_{\mathbf{Q}}}{m^2\omega}(\mathbf{q}\cdot\mathbf{Q})[\mathbf{q}\cdot(\mathbf{p}-\mathbf{k}-\mathbf{Q})]. \tag{30}$$

As is to be expected (and indeed shown to be the case in Appendix C 1), a typical value of $|\mathbf{k}-\mathbf{p}| \sim k_{\mathrm{F}} \gg Q \gtrsim \kappa$. Then $\mathcal{A}_2$ can be estimated as $|\mathcal{A}_2| \sim q^2 Q k_{\mathrm{F}} V_Q/m^2\omega$. The resultant integral over Q is convergent at $Q = 0$ but needs to be cut off at $Q \sim k_{\mathrm{F}}$ at the upper limit, upon which one reproduces the structure of Eq. (5). (The cross-term, $\mathcal{A}_1\mathcal{A}_2$, vanishes to leading order upon angular integration.)

We pause here to emphasize a nontrivial structure of the expansion in $1/\omega$. Indeed, the expansion of the individual components in Eq. (23) starts with the $1/\omega$ terms, which cancel each other, followed by the $O(\mathbf{v}_{\mathbf{k},\mathbf{p}}\cdot\mathbf{q}/\omega^2)$ terms, which are supposed to be the leading ones. However, the latter also almost cancel each other, and one needs to keep two $O(q^2)$ terms: the $q^2/2m$ terms in Eq. (28b) and the entire $\mathcal{A}_2$ term in Eq. (28c). For $\omega \ll \omega_{\mathrm{p}}(\kappa)$, the "new" term ($\mathcal{A}_2$) exceeds the "old" one.

Deferring further details to Appendix C 1, we present here the final result for the optical conductivity of a 2DEG with parabolic dispersion:

$$\mathrm{Re}\sigma(q,\omega) = \frac{e^2}{48\pi^2}\frac{q^2}{k_{\mathrm{F}}^2}\left(1 + 4\pi^2\frac{T^2}{\omega^2}\right)\ln\frac{v_{\mathrm{F}}\kappa}{\max\{|\omega|, 2\pi T\}} + \frac{e^2}{24\pi^2}\frac{q^2\kappa^2}{m^2\omega^2}\left(1 + 4\pi^2\frac{T^2}{\omega^2}\right)\ln\frac{k_{\mathrm{F}}}{\kappa}. \tag{31}$$

The second ("new") term coincides with Eq. (5), which confirms the conjecture made in Refs. [8,9], while the second one is subleading to the first one for $\omega \ll \omega_{\mathrm{p}}(\kappa)$.

C. Three-dimensional electron gas

For a 3D electron gas with parabolic dispersion, the form of $\mathcal{A}$ is the same as in Eqs. (28a)–(30), but the integrals are different due to a change in the phase space. Deferring the details to Appendix C 2, we present here only the final result for the optical conductivity in the limit of $\omega \ll v_F\kappa$:

$$\mathrm{Re}\sigma(q,\omega) = \frac{e^2\kappa}{720}\frac{q^2\kappa^2}{m^2\omega^2}\left(1+4\pi^2\frac{T^2}{\omega^2}\right), \tag{32}$$

where the inverse screening length is given by $\kappa^2 = 8\pi e^2 N_F$ and $N_F = mk_F/2\pi^2$ is the density of states per spin.

D. Doped monolayer graphene

The optical conductivity of graphene was calculated in Refs. [8,9], but the most complete result was given in Ref. [9] without a derivation. Here, we rederive this result using the MRG method.

Without loss of generality, we assume that the Fermi energy is located in the upper Dirac cone. In the low-energy limit, i.e., for $\max\{\omega, T\} \ll E_F$, one can neglect the presence of the lower Dirac cone [29]. Also, for a long-range Coulomb interaction, one can neglect processes that lead to swapping of electrons between the K and K' valleys, as well as the exchange parts of both intra- and intervalley scattering amplitudes. For the same reason, the phase factors in the matrix elements between spinor states can be replaced by unities. With all these simplifications, electrons in graphene can be described by the following low-energy Hamiltonian:

$$H_0 = \sum_{\varsigma,\mathbf{k},s}(v_D k - E_F)c^\dagger_{\varsigma,\mathbf{k},s}c_{\varsigma,\mathbf{k},s} + \frac{1}{2}\sum_{\mathbf{k},\mathbf{p},\mathbf{Q}}\sum_{s,s',\varsigma,\varsigma'} V^{(0)}_{\mathbf{Q}} \times c^\dagger_{\varsigma,\mathbf{k}+\mathbf{Q},s}c^\dagger_{\varsigma',\mathbf{p}-\mathbf{Q},s'}c_{\varsigma',\mathbf{p},s'}c_{\varsigma,\mathbf{k},s} \tag{33}$$

where $\varsigma = \pm 1$ labels the K and K' valleys, $\mathbf{k}$ is the electron momentum measured from the center of the corresponding valley, $s = \pm 1$ is the spin projection, and $V^{(0)}_{\mathbf{Q}} = 2\pi e^2/Q$ is the bare Coulomb potential. Within this approximation, the valley index plays the role of a conserved isospin. Therefore the optical conductivity can be calculated by applying the MRG method to the case of spin-1/2 fermions occupying a single valley, i.e., using Eq. (24) and then multiplying the result by $2^2 = 4$.

In contrast to 2D and 3D electron gases, graphene is a non-Galilean-invariant system. Therefore its optical conductivity is finite even at $q = 0$. However, we will see that in order to determine the plasmon linewidth accurately, one needs to retain both $O(1)$ and $O(q^2)$ terms in the optical conductivity. Recalling the factor of $1/q^2$ in Eq. (24), we see that $\mathcal{A}$ should have terms of $O(q)$ and $O(q^2)$, which would give the $O(1)$ and $O(q^2)$ contributions to the conductivity, respectively. As shown in Appendix C 3, the result for $\mathcal{A}$ to required accuracy is given by

$$\mathcal{A} = \mathcal{A}_1 + \mathcal{A}_2, \tag{34a}$$

$$\mathcal{A}_1 = -V_{\mathbf{Q}}\frac{qv_D}{E_F}[(\varepsilon_{\mathbf{p}} - \varepsilon_{\mathbf{p}-\mathbf{Q}})\cos\theta_{\mathbf{qp}} + (\varepsilon_{\mathbf{k}} - \varepsilon_{\mathbf{k}+\mathbf{Q}})\cos\theta_{\mathbf{qk}}], \tag{34b}$$

$$\mathcal{A}_2 = V_{\mathbf{Q}}\frac{q^2 v_D}{2k_F}\left[\frac{1}{2}\sin^2\theta_{\mathbf{pq}} + 2\frac{v_D Q}{\omega}(F_{\mathbf{p}} - F_{\mathbf{k}})\right], \tag{34c}$$

where

$$F_{\mathbf{k}} = \cos\theta_{\mathbf{qk}}(\cos\theta_{\mathbf{qQ}} - \cos\theta_{\mathbf{qk}}\cos\theta_{\mathbf{kQ}}),$$

$F_{\mathbf{p}}$ is obtained by interchanging $\mathbf{k}$ and $\mathbf{p}$ in $F_{\mathbf{k}}$, and $\theta_{\mathbf{nn}'}$ denotes the angle between the vectors $\mathbf{n}$ and $\mathbf{n}'$.

The q-independent part of Reσ is exactly the same as calculated in Ref. [9], and we will give only a brief summary of the computational steps. Once $\mathcal{A}_1^2$ is substituted into Eq. (24), the differences of electronic dispersions in Eq. (34c) can be expressed via the frequencies ω and Ω, using the constraints imposed by the delta functions in Eq. (24). Suppose that $T = 0$. Then, given that $\Omega \sim \omega$, we have $\mathcal{A}_1^2 \propto \omega^2$. The three energy integrations (over $\varepsilon_{\mathbf{k}}$, $\varepsilon_{\mathbf{p}}$, and Ω) are effectively constrained to the interval $(0, \omega)$ by the Fermi functions and therefore contribute a factor of ω each. Altogether, it follows that $\mathrm{Re}\sigma_1(\omega) \propto \omega^2 \times \omega^3/\omega^3 = \omega^2$. This is the leading contribution to the conductivity for $\omega \ll E_F$. Therefore one can neglect the frequencies in the delta functions, upon which they impose purely geometric constraints on the angular variables; for $Q \ll k_F$, we simply have $\cos\theta_{\mathbf{pQ}} = \cos\theta_{\mathbf{kQ}} = 0$. The Q integration is the same as that for a 2DEG (see Appendix C 1): Given that each of the two delta functions gives a factor of $1/Q$, the integral over Q diverges logarithmically at the lower limit. Cutting this divergence off at $Q = |\omega|/v_D$, we reproduce the $T = 0$ limit of Eq. (4b). The reasoning for the opposite limit of $\omega \ll T$ is essentially the same, except for now the dispersions in $\mathcal{A}_1^2$ give a factor of T^2, another T^3 comes from the energy integrations, and the factor of $1 - e^{-\omega/T}$ in Eq. (24) is reduced to ω/T. Cutting off the Q integration at $Q = T/v_D$, we obtain $\mathrm{Re}\sigma_1(\omega) \propto (\omega/T) \times T^5 \times \ln T/\omega^3 = T^4 \ln T/\omega^2$, which is the $\omega \ll T$ limit of Eq. (4b). Details of calculating the $O(q^2)$ term can be found in Appendix C 3, and the final result is given by Eqs. (4a)–(4c).

IV. PHYSICAL INTERPRETATION

To clarify the physical meaning of the results obtained in the previous sections, we start from the relation between the real part of the conductivity and the viscosities of the electron liquid [31]. This relation can be inferred from the equation of motion for the current density and has the form

$$\mathrm{Re}\sigma(q,\omega) = e^2\frac{nq^2}{m\omega^2}\left[\nu_L + \left(2 - \frac{2}{D}\right)\nu_T\right], \tag{35}$$

where $\nu_L = \zeta/nm$ and $\nu_T = \eta/nm$ are the bulk and shear viscosities, respectively (also known as longitudinal and transverse kinematic viscosities, respectively), of the electron gas with number density n, evaluated in the collisionless regime (not to be confused with the hydrodynamic viscosities, which are nonperturbative in the Coulomb interaction).

Interestingly, Eq. (35) can be viewed as an extension of the Einstein relation for the conductivity. The standard Einstein relation (for electrons in the presence of impurities) reads

$$\sigma = e^2 N(0)\mathcal{D}, \tag{36}$$

where $N(0) = \lim_{q\to 0}\chi_c(q,0)$ is the density of states at the Fermi level, $\chi_c(q,\omega)$ is the charge susceptibility, and $\mathcal{D}$

is the diffusion coefficient. Equation (35) can be obtained by replacing $N(0) = \lim_{q\to 0} \chi_c(q, 0)$ with $\lim_{q\to 0} \chi_c(q, \omega) = -nq^2/m\omega^2$ at finite frequency (notice, however, the change of sign in front of χ_c) and replacing $\mathcal{D}$ with $\nu_L + (2 - 2/D)\nu_T$, which is the diffusion coefficient of the momentum density.

The key question now is: What is the low-frequency behavior of the transport coefficients ν_L and ν_T? The answer is that ν_T tends to a finite value at $\omega \to 0$ (plus corrections of order ω^2), while ν_L vanishes at $\omega \to 0$ as ω^2. Thus we see that the terms proportional to ω^{-2} arise from the shear viscosity, while the ω-independent terms arise from the ω^2 contributions to the shear viscosity as well as the bulk viscosity. (We stress that this is valid in dimensions $D > 1$, where a transverse viscosity can be defined.)

What is the physical reason for the difference? The two viscosity coefficients can be expressed in terms of the stress-stress response function as follows:

$$\nu_L(\omega) = -\frac{1}{D^2}\frac{\mathrm{Im}\langle\langle \hat{P}_{\mu\mu}; \hat{P}_{\nu\nu}\rangle\rangle_\omega}{nm\omega} \tag{37}$$

and

$$\nu_T(\omega) = -\frac{\mathrm{Im}\langle\langle \hat{P}_{xy}; \hat{P}_{xy}\rangle\rangle_\omega}{nm\omega}, \tag{38}$$

where

$$\langle\langle \hat{A}; \hat{B}\rangle\rangle_\omega \equiv -i\int_0^\infty dt\, \langle[\hat{A}(t), \hat{B}(0)]\rangle e^{i(\omega+i0^+)t}, \tag{39}$$

$[\cdot,\cdot]$ is the commutator of two operators, and $\langle\cdot\rangle$ denotes the statistical average over the equilibrium density matrix. The time evolution of $\hat{A}$ is generated by the noninteracting Hamiltonian. The spectral density of an observable $\hat{O}$ is obtained from Eq. (39) by calculating $\mathrm{Im}\langle\langle \hat{O}; \hat{O}\rangle\rangle_\omega$. Furthermore, the stress-tensor operator is given by [32]

$$\hat{P}_{\mu\nu} = \hat{T}_{\mu\nu} + \hat{W}_{\mu\nu}, \tag{40}$$

where

$$\hat{T}_{\mu\nu} = \sum_{\mathbf{k}} \frac{k_\mu k_\nu}{m} \hat{a}^\dagger_{\mathbf{k}} \hat{a}_{\mathbf{k}}, \tag{41}$$

$$\hat{W}_{\mu\nu} = \frac{1}{2}\sum_{\mathbf{k},\mathbf{Q}} \left(\frac{Q_\mu Q_\nu}{Q}\frac{dV_Q^{(0)}}{dQ} + \delta_{\mu\nu} V_Q^{(0)} \right) \hat{a}^\dagger_{\mathbf{k}} \hat{n}^\dagger_{\mathbf{Q}} \hat{a}_{\mathbf{k}-\mathbf{Q}}, \tag{42}$$

$V_Q^{(0)}$ is the bare Coulomb potential, and $\hat{n}_{\mathbf{Q}} = \sum_{\mathbf{p}} \hat{a}^\dagger_{\mathbf{p}-\mathbf{Q}} \hat{a}^\dagger_{\mathbf{p}}$ is the number density operator.

Let us consider the bulk viscosity first. The trace of the stress tensor is easily seen to be given by $\hat{P}_{\mu\mu} = \hat{T} + \hat{H}$, where $\hat{T}$ is the kinetic energy operator and $\hat{H}$ is the total Hamiltonian of the electron system, i.e., the sum of the kinetic and interaction parts. $\hat{H}$ is a constant of the motion and thus does not contribute to the response function.

Then we are left with

$$\nu_L(\omega) = -\frac{1}{D^2}\frac{\mathrm{Im}\langle\langle \hat{T}; \hat{T}\rangle\rangle_\omega}{nm\omega}, \tag{43}$$

which can be rewritten in terms of the time derivatives of $\hat{T}$ as

$$\nu_L(\omega) = -\frac{1}{D^2}\frac{\mathrm{Im}\langle\langle \dot{\hat{T}}; \dot{\hat{T}}\rangle\rangle_\omega}{nm\omega^3}, \tag{44}$$

where we used that

$$\begin{aligned} i\omega\langle\langle \hat{A}; \hat{B}\rangle\rangle_\omega &= i\langle[\hat{A}, \hat{B}]\rangle - \langle\langle \dot{\hat{A}}; \hat{B}\rangle\rangle_\omega \\ &= i\langle[\hat{A}, \hat{B}]\rangle + \langle\langle \hat{A}; \dot{\hat{B}}\rangle\rangle_\omega. \end{aligned} \tag{45}$$

The second line of this equation follows from time-translational invariance of the response function. Equation (44) is obtained by noting that the commutator of two Hermitian operators is anti-Hermitian, and therefore all its eigenvalues are imaginary. Thus the term $i\langle[\hat{T}, \hat{T}]\rangle$, obtained by applying Eq. (45) to $\langle\langle \hat{T}; \hat{T}\rangle\rangle_\omega$ twice, is purely real and can only contribute to the real part of the response function.

Due to the Coulomb interaction, the kinetic energy operator depends on time, and its time derivative is given by

$$\dot{\hat{T}} = -i\sum_{\mathbf{Q}} V_Q^{(0)} (\mathbf{Q}\cdot\hat{\mathbf{j}}_{-\mathbf{Q}})\hat{n}_{\mathbf{Q}}. \tag{46}$$

(Notice that $\dot{\hat{T}}$ is proportional to the scalar product of the Coulomb force density $\hat{\mathbf{F}}_{\mathbf{Q}} = -i\mathbf{Q}V_Q^{(0)}\hat{n}_{\mathbf{Q}}$ and the *longitudinal* current density $\hat{\mathbf{j}}_{-\mathbf{Q}}$.)

In the limit of a large number of fermion flavors [33] the spectral function $\mathrm{Im}\langle\langle \dot{\hat{T}}; \dot{\hat{T}}\rangle\rangle_\omega$ is the convolution of two electron-hole spectral functions, associated with density fluctuations and longitudinal current density fluctuations, respectively. The spectral function of density fluctuations vanishes as ω at $\omega \to 0$, while that of longitudinal current density fluctuations vanishes as ω^3, as one can see from the well-known relation $\mathrm{Im}\langle\langle \mathbf{Q}\cdot\hat{\mathbf{j}}_{\mathbf{Q}}; \mathbf{Q}\cdot\hat{\mathbf{j}}_{-\mathbf{Q}}\rangle\rangle_\omega = \omega^2 \mathrm{Im}\chi_c(Q, \omega)$ [17]. Therefore at zero temperature we have

$$\mathrm{Im}\langle\langle \dot{\hat{T}}; \dot{\hat{T}}\rangle\rangle_\omega \sim \int_0^\omega d\Omega\Omega^3(\omega - \Omega) \propto \omega^5. \tag{47}$$

Substituting the last result into Eq. (44) gives $\nu_L \propto \omega^2$ as announced. The essential reason for this result is the scarcity of longitudinal electron-hole pair excitations at low frequency: Their spectral density vanishes as ω^3.

Let us now consider the shear viscosity, Eq. (38). Without loss of generality we can orient the x axis along $\mathbf{Q}$ and the y axis perpendicular to $\mathbf{Q}$. It can be easily shown that the averages $\langle\langle \hat{W}_{xy}; \hat{W}_{xy}\rangle\rangle_\omega$ and $\langle\langle \hat{T}_{xy}; \hat{W}_{xy}\rangle\rangle_\omega$ involve only longitudinal current density fluctuations and, therefore, vanish as ω^2 as before. However, the average $\langle\langle \hat{T}_{xy}; \hat{T}_{xy}\rangle\rangle_\omega$ now involves transverse current density fluctuations. As before, we rewrite $\nu_T(\omega)$ as

$$\nu_T(\omega) = -\frac{1}{D^2}\frac{\mathrm{Im}\langle\langle \dot{\hat{T}}_{xy}; \dot{\hat{T}}_{xy}\rangle\rangle_\omega}{nm\omega^3} \tag{48}$$

and note that

$$\dot{\hat{T}}_{xy} = -i\sum_{\mathbf{Q}} V_Q^{(0)} (Q_x \hat{j}_{Ty,-\mathbf{Q}}\hat{n}_{\mathbf{Q}} + Q_y \hat{j}_{Tx,-\mathbf{Q}}\hat{n}_{\mathbf{Q}}) + \cdots, \tag{49}$$

where $\hat{j}_{Ty,-\mathbf{Q}}$ is the y component of the transverse current density (i.e., parallel to y and perpendicular to $\mathbf{Q}$) and $\cdots$ stands for subleading terms that contain the longitudinal component of the current density operator. Now we see that the spectral function $\mathrm{Im}\langle\langle \dot{\hat{T}}_{xy}; \dot{\hat{T}}_{xy}\rangle\rangle_\omega$ is the convolution of two electron-hole spectral functions, one associated with density fluctuations and the other one associated with *transverse* current density fluctuations. The spectral density of transverse

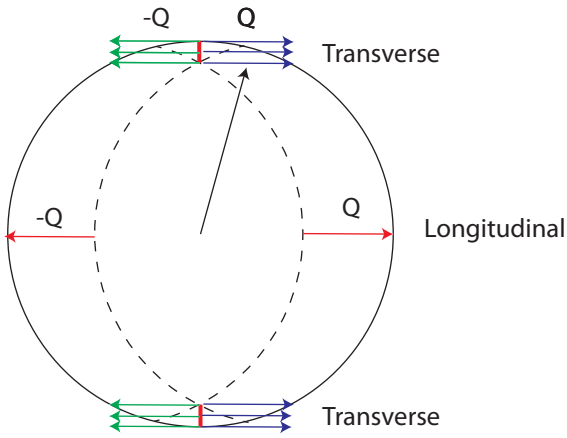

FIG. 1. The horizontal arrows represent the momenta of low-energy electron-hole pair excitations, $\mathbf{Q}$ and $-\mathbf{Q}$. Such excitations contribute to plasmon damping. Due to kinematic constraints, the initial momenta of the excited electrons are confined to the crescent-shaped regions (external to the dashed lines), within the Fermi surface (solid circle). The short red segments denote the widths of allowed regions of the initial momenta for excitations of a given (small) energy. Notice that these excitations are essentially transverse, meaning that the average momentum of the initial and final state of the excited electron (black arrow) is almost orthogonal to the momentum of the excitation, $\mathbf{Q}$. The size of the integration region (red segments) vanishes linearly as the energy of the excitation tends to zero, consistent with the fact that the spectral function of density fluctuations vanishes linearly at low frequency. By contrast, longitudinal current excitations with the same wave vector $\mathbf{Q}$ (indicated by the red horizontal arrows) have much higher energies: Their contribution to the low-frequency spectrum vanishes as the third power of the excitation energy.

current density fluctuations vanishes as ω as opposed to ω^3. Therefore we now have

$$\mathrm{Im}\langle\langle \dot{\hat{T}}_{xy}; \dot{\hat{T}}_{xy}\rangle\rangle_{\omega} \sim \int_0^{\omega} d\Omega\Omega(\omega-\Omega) \propto \omega^3. \tag{50}$$

Substituting the last result into Eq. (48) gives a finite value of ν_T in the $\omega \to 0$ limit.

The reason for the different behavior of the longitudinal and transverse current spectral functions is illustrated in Fig. 1.

V. PLASMON LINEWIDTH

A. Definitions

We now derive the expressions for the plasmon linewidth, using the results for $\mathrm{Re}\sigma(q,\omega)$ obtained in previous sections. The linewidth, $\Gamma(q)$, is calculated at the plasmon pole and is given by

$$\Gamma(q) = \pi q\, \mathrm{Re}\sigma(q,\omega)|_{\omega=\omega_{\mathrm{p}}(q)} \tag{51}$$

in 2D and

$$\Gamma(q) = 2\pi\, \mathrm{Re}\sigma(q,\omega)|_{\omega=\omega_{\mathrm{p}}(q)} \tag{52}$$

in 3D. It is also customary to define a dimensionless inverse quality factor (IQF)

$$\gamma(q) = \frac{2\Gamma(q)}{\omega_{\mathrm{p}}(q)}. \tag{53}$$

B. Electron gas with parabolic dispersion

1. 2D electron gas

In a 2DEG, the plasmon frequency is $\omega_{\mathrm{p}}(q) = v_{\mathrm{F}}\sqrt{\kappa q/2}$ with $\kappa = 2me^2$. Substituting the leading term in the optical conductivity [Eq. (5)] into Eq. (51), we obtain the plasmon linewidth as

$$\Gamma(q) = \frac{e^2}{12\pi} \ln\frac{k_{\mathrm{F}}}{\kappa} \frac{q^2\kappa}{k_{\mathrm{F}}^2}\left(1 + 4\pi^2\frac{T^2}{\omega_{\mathrm{p}}^2(q)}\right). \tag{54}$$

Defining $T_{\mathrm{p}} \equiv v_{\mathrm{F}}\kappa \sim \omega_{\mathrm{p}}(\kappa)$, we see that $\Gamma(q)$ behaves as qT^2 for $q \ll \kappa(T/T_{\mathrm{p}})^2$ and as q^2 for $q \gg \kappa(T/T_{\mathrm{p}})^2$. The corresponding IQF can be written in a dimensionless form as

$$\gamma(q) = \frac{2\sqrt{2}}{3\pi}\alpha_{\mathrm{e}}^3 \ln\frac{1}{\alpha_{\mathrm{e}}} \bar{q}^{3/2}\left(1 + \frac{8\pi^2\bar{T}^2}{\bar{q}}\right), \tag{55}$$

where $\alpha_{\mathrm{e}} = e^2/v_{\mathrm{F}}$ is the dimensionless coupling constant of the Coulomb interaction, $\bar{q} = q/\kappa$, and $\bar{T} = T/T_{\mathrm{p}}$.

2. 3D electron gas

Neglecting the q-dependent part of the plasmon dispersion, the plasmon frequency of a 3D electron gas is given by $\omega_{\mathrm{p}} = \sqrt{4\pi ne^2/m}$, where $n = k_{\mathrm{F}}^3/\pi^2$ is the number density. Substituting $\mathrm{Re}\sigma$ from Eq. (32) into Eq. (52), we obtain

$$\Gamma(q) = \frac{\pi e^2\kappa}{360}\frac{q^2\kappa^2}{m^2\omega_{\mathrm{p}}^2}\left(1 + 4\pi^2\frac{T^2}{\omega_{\mathrm{p}}^2}\right), \tag{56}$$

where $\kappa^2 = 8\pi e^2 N_{\mathrm{F}}$ with $N_{\mathrm{F}} = mk_{\mathrm{F}}/2\pi^2$, and

$$\gamma(q) = \frac{\sqrt{3}}{15}\alpha_{\mathrm{e}}^2\bar{q}^2(1 + 12\pi^2\bar{T}^2), \tag{57}$$

where the dimensionless parameters are the same as those defined after Eq. (55). The asymptotic forms of $\Gamma(q)$ and $\gamma(q)$ are the same as for a 2DEG.

C. Doped monolayer graphene

So far, we discussed graphene in the isotropic approximation, which neglects trigonal warping of the Fermi surfaces around the K and K' points. The corresponding optical conductivity is given by the sum of $\mathrm{Re}\sigma_1$ and $\mathrm{Re}\sigma_2$ from Eqs. (4b) and (4c), respectively. Trigonal warping breaks the degeneracy of the K and K' valleys, and intervalley scattering is now allowed to contribute to the conductivity, even if there is no swapping of electrons between the valleys. The corresponding contribution to the conductivity was found in Ref. [9]:

$$\mathrm{Re}\sigma_3(\omega) = \frac{29e^2}{48\pi^2}\frac{e^2}{v_{\mathrm{D}}} \ln\frac{k_{\mathrm{F}}}{\kappa}(k_{\mathrm{F}}a)^2\left(1 + 4\pi^2\frac{T^2}{\omega^2}\right), \tag{58}$$

where a is the distance between two nearest carbon atoms. This contribution is of a regular FL type [20], i.e., it is finite at $q = 0$ and, in contrast to $\mathrm{Re}\sigma_1$, is not suppressed due to partial Galilean invariance. However, being a lattice effect, it

becomes significant only at sufficiently high filling, when the product $k_F a$ is not too small.

Accordingly, the plasmon linewidth is written as the sum of three parts:

$$\Gamma(q) = \Gamma_1(q) + \Gamma_2(q) + \Gamma_3(q), \tag{59a}$$

$$\Gamma_1(q) = \frac{\pi e^2}{480}\frac{q^2\kappa}{k_F^2}\left(1 + 4\pi^2\frac{T^2}{\omega_p^2(q)}\right) \times \left(3 + 8\pi^2\frac{T^2}{\omega_p^2(q)}\right)\ln\frac{v_D\kappa}{\max\{\omega_p(q), T\}}, \tag{59b}$$

$$\Gamma_2(q) = \frac{e^2}{12\pi}\frac{q^2\kappa}{k_F^2}\ln\frac{k_F}{\kappa}\left(1 + 4\pi^2\frac{T^2}{\omega_p^2(q)}\right), \tag{59c}$$

$$\Gamma_3(q) = \frac{29e^2}{48\pi}\frac{e^2 q}{v_D}\ln\frac{k_F}{\kappa}(k_F a)^2\left(1 + 4\pi^2\frac{T^2}{\omega_p^2(q)}\right), \tag{59d}$$

where $\omega_p(q) = v_D\sqrt{\kappa q/2}$ is the plasmon frequency and $\kappa = 4e^2 k_F/v_D$. For $q \ll \kappa\sqrt{T/T_p}$, the linewidth is determined primarily by $\Gamma_1(q)$ in Eq. (59b), which is independent of q and scales as $T^4 \ln T$ in this limit. In the opposite limit of $q \gg \kappa\sqrt{T/T_p}$, the contributions from Γ_1 and Γ_2 are of the same order of magnitude (although Γ_2 is numerically smaller), and both scale as q^2. On the other hand, the contribution from Γ_3 is much smaller than that from Γ_1 for any reasonable value of $k_F a$.

In terms of the dimensionless variables introduced after Eq. (55), the IQF for graphene is written as

$$\gamma(q) = \gamma_1(q) + \gamma_2(q) + \gamma_3(q), \tag{60a}$$

$$\gamma_1(q) = \frac{2\Gamma_1(q)}{\omega_p(q)} = \frac{\sqrt{2}\pi}{15}\bar{q}^{3/2}\alpha_g^3\left(1 + \frac{8\pi^2\bar{T}^2}{\bar{q}}\right) \times \left(3 + \frac{16\pi^2\bar{T}^2}{\bar{q}}\right)\ln\frac{1}{\max\{\bar{q}, \sqrt{\bar{T}}\}}, \tag{60b}$$

$$\gamma_2(q) = \frac{2\Gamma_2(q)}{\omega_p(q)} = \frac{4\sqrt{2}}{3\pi}\bar{q}^{3/2}\alpha_g^3\ln\frac{1}{\alpha_g}\left(1 + \frac{8\pi^2\bar{T}^2}{\bar{q}}\right), \tag{60c}$$

$$\gamma_3(q) = \frac{2\Gamma_3(q)}{\omega_p(q)} = \frac{29\sqrt{2}}{24\pi}\bar{q}^{1/2}\alpha_g^2\ln\frac{1}{\alpha_g}(k_F a)^2\left(1 + \frac{8\pi^2\bar{T}^2}{\bar{q}}\right), \tag{60d}$$

where $\alpha_g = e^2/v_D$.

D. Discussion

The IQFs for 2D and 3D electrons gases are plotted as a function of $\bar{q} = q/\kappa$ in Fig. 2. All other parameters being equal, damping is stronger in 2D (solid curve) than in 3D (dashed line) over a wide range of q. This is primarily due to the fact that finite temperature has little effect on damping in 3D. Indeed, the temperature dependence of $\gamma(q)$ in Eq. (57) is weak as long as $\bar{T} \ll 1$ (or $T \ll \omega_p$), and $\gamma(q)$ scales as $\bar{q}^2$ for any $\bar{q}$. In contrast, $\gamma(q)$ in 2D [Eq. (55)] decreases with $\bar{q}$ more slowly than in 3D, i.e., as $\bar{q}^{1/2}\bar{T}^2$ for $\bar{q} \ll \bar{T}^2$ (or $q \ll \kappa\sqrt{T/T_p}$). As $\bar{q}$ approaches 1 from below, damping in 2D and 3D becomes comparable.

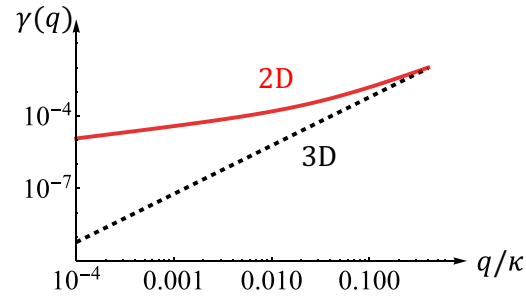

FIG. 2. Inverse qualify factor, $\gamma(q)$ [Eq. (53)], for 2D (solid curve) and 3D (dashed curve) electron gases as a function of q/κ, where κ is the inverse screening radius. The electron temperature is $T = 0.02\, v_F\kappa$, where v_F is the Fermi velocity, and the coupling constant of the Coulomb interaction is $\alpha = e^2/v_F = 0.7$.

The partial components of $\gamma(q)$ as well as total $\gamma(q)$ in graphene are plotted in Fig. 3. First, we note that $\gamma_1(q)$ dominates over the other two components for the entire range of q. Next, we see that the effect of finite temperature on damping in graphene is even stronger than for a 2DEG: For $\bar{q} \ll 1$, $\gamma(q) \approx \gamma_1(q)$ scales as $\bar{T}^4/\sqrt{\bar{q}}$, i.e., the (relative) plasmon linewidth *decreases* with increasing $\bar{q}$. In this regime, the usual numerical prefactor of 2π, amplifying the effect of finite temperature on collective modes, plays a very important role, as it leads to an enhancement of the linewidth by a factor of $2(2\pi)^4 \approx 3120$. An apparent divergence of $\gamma(q)$ at $q \to 0$ signals a breakdown of the collisionless approximation and a crossover to the hydrodynamic regime. As q increases, $\gamma(q)$ goes through a shallow minimum at $\bar{q} = (4\pi^2(\sqrt{13} - 2)/9)\bar{T}^2 \approx 7.0\bar{T}^2$ and then increases as $\bar{q}^{3/2}$. Comparing the vertical scales of Figs. 2 and 3, we see that, all other parameters being equal, damping is, in general, stronger in graphene than in an electron gas with parabolic dispersion, even though the IQF for the latter is higher order in the coupling constant (third vs second). This is, again, due to a higher sensitivity of

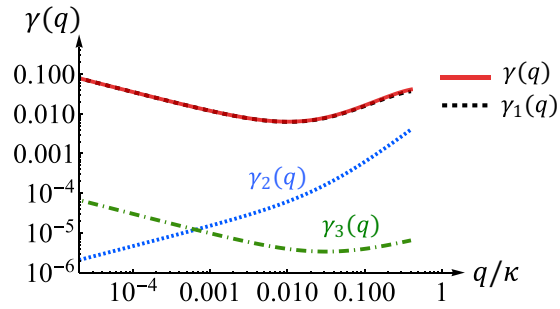

FIG. 3. Inverse qualify factor, $\gamma(q)$ [Eq. (53)], for doped monolayer graphene as a function of q/κ, where κ is the inverse screening radius. $\gamma_1(q)$ (dashed curve), γ_2 (dotted curve), and γ_3 (dash-dotted curve) are the partial components of total $\gamma(q)$ (solid curve), as defined by Eqs. (60a)–(60d). The electron temperature $T = 0.02\, v_D\kappa$, where v_D is the Dirac velocity, the filling factor $k_F a = 0.01$, and the coupling constant of the Coulomb interaction $\alpha_g = e^2/v_D = 0.7$, which corresponds to the case of monolayer graphene mounted on a semi-infinite boron nitride substrate.

the linewidth of graphene to finite T. For $\bar{q} \ll \bar{T}^2$, the ratio $\gamma(q)|_{\text{2DEG}}/\gamma(q)|_{\text{graphene}} \sim \bar{q}/\bar{T}^2 \ll 1$.

Damping of plasmons in graphene at finite T was discussed by Lucas and Das Sarma [14], who conjectured that $\Gamma(q) \propto qT^2$ in the collisionless regime. This result is consistent with Eq. (54) for a 2DEG with parabolic dispersion and with the subleading, $\Gamma_2(q)$ contribution to the linewidth in graphene [Eq. (59c)]. However, the leading contribution to the linewidth in graphene is given by $\Gamma_1(q)$ [Eq. (59b)], which is independent of q and scales as $T^4 \ln T$ for small $q \ll \kappa(T/T_{\text{p}})^2$. The discrepancy between our result and that of Ref. [14] is due to the assumption of Ref. [14] that the relevant relaxation rate in graphene scales in a canonical FL way, i.e., as T^2. However, whereas the single-particle relaxation rate in graphene indeed scales as T^2 (modulo a factor of $\ln T$), the current relaxation rate, defined as $\text{Re}\sigma = ne^2/m^*\omega^2\tau_{\text{j}}(\omega, T)$ with n being the carrier number density, scales as $1/\tau_{\text{j}} \propto \max\{\omega^4 \ln|\omega|, T^4 \ln T\}$; see, e.g., Ref. [27] and references therein. This property is not unique to graphene, but common for any 2D or 3D FL with an isotropic but nonparabolic spectrum (except that there is no $\ln T$ factor in 3D) [9,30].

VI. CONCLUSIONS

Prompted by some discrepancies between results of different theoretical papers, we revisited the optical conductivity, $\text{Re}\sigma(q, \omega)$, of an electron system due to electron-electron interaction and a related issue of plasmon damping, focusing on the collisionless (as opposed to hydrodynamic) regime. Setting aside more sophisticated methods, we first showed that a semiclassical Boltzmann equation for a two-dimensional electron gas (2DEG) with parabolic dispersion yields the optical conductivity which behaves as q^2T^2/ω^4 for $v_{\text{F}}q \ll \omega \ll T$. This behavior is consistent with the results of Refs. [8,9] but not with those of Ref. [10]. Next, we rederived the full expression for $\text{Re}\sigma(q, \omega)$ of a 2DEG [Eq. (5)], using the original and elegant method of Ref. [10], and identified the reason for the discrepancy between the result of Ref. [10] and the results of Refs. [8,9]. We showed that the results of Ref. [10] and Refs. [8,9] correspond to physically distinct contributions, arising from the bulk and shear viscosities of an electron liquid. While the bulk viscosity vanishes at $\omega \to 0$, the shear one approaches a finite value. This explains why at sufficiently low frequency, the conductivity found in Refs. [8,9] is larger than the one found in Ref. [10]. For completeness, we also calculated $\text{Re}\sigma(q, \omega)$ of a 3D electron gas and doped graphene, using the same method. The optical conductivity of a 3D electron gas [Eq. (32)] is found to be similar to the optical conductivity in the 2D case: In both cases, $\text{Re}\sigma(q, \omega)$ vanishes at $q \to 0$ due to Galilean invariance. However, the case of doped graphene is different due to broken Galilean invariance. As a result, $\text{Re}\sigma(q, \omega)$ is finite at $q = 0$ and scales as $\omega^2 \ln|\omega|$ at $T = 0$. This result was derived in our previous work [9], using the equations-of-motion method. Here, we also rederived the $O(q^2)$ term in the conductivity and found that it is exactly the same as in a 2D electron gas (up to a redefinition of an effective electron mass), in agreement with a conjecture of Refs. [8,9].

Using our results for the optical conductivity, we analyzed the behavior of the plasmon linewidth, $\Gamma(q)$, in various systems. Given that the electron temperature in an experiment may be significantly higher than the lattice one, we paid special attention to the T dependence of $\Gamma(q)$. We found that, all parameters being equal, the effect of finite T on plasmon damping is the strongest in graphene: $\Gamma(q)$ is independent of q and scales as $T^4 \ln T$ for $q \ll T^2/v_{\text{D}}^2\kappa$, where v_{D} is the Dirac velocity and κ is the inverse screening length. This scaling reflects the fact that the current relaxation rate in a non-Galilean-invariant but isotropic system behaves as $\max\{\omega^4, T^4\}$ (with an extra $\ln\max\{|\omega|, T\}$ factor in 2D) [9,30]. We remind the reader that our results are valid in the collisionless regime, i.e., for $\omega\tau_{\text{j}}(\omega = 0, T) \gg 1$. For example, $1/\tau_{\text{j}}(\omega = 0, T) \sim T^4 \ln(E_{\text{F}}/T)/E_{\text{F}}^3$ for graphene.

To compare with experiment, we focus on the near-field-spectroscopy study described in Ref. [2], in which the dispersion and linewidth of plasmons were measured in monolayer graphene encapsulated by hexagonal boron nitride (hBN). A subsequent theoretical calculation [33] showed that the primary damping mechanism is scattering by graphene acoustic phonons. Using the effective dielectric constant for graphene between two semi-infinite slabs of hBN, $\epsilon^* \approx 5.0$ [33], we obtain $\alpha_{\text{g}} = 0.43$. Correspondingly, $\omega_{\text{p}} = 66\,\text{meV}$ at $n = 7.2 \times 10^{12}\ \text{cm}^{-2}$ and $q = 0.25 \times 10^6\ \text{cm}^{-1}$, and according to Fig. 5 of Ref. [33], the inverse plasmon lifetime due to electron-phonon interaction is $1/\tau_{\text{eph}} \approx 3.0 \times 10^{12}\ \text{s}^{-1}$ at room temperature. Using the same parameters, we obtain from Eqs. (59a)–(59d) for the inverse plasmon lifetime due to electron-electron interaction $1/\tau_{\text{ee}} = 2\Gamma \approx 1.5 \times 10^{12}\ \text{s}^{-1}$, which is smaller than $1/\tau_{\text{eph}}$ only by a factor of 2. (We remind the reader that the dominant contribution to Γ is given by Γ_1.) Furthermore, $1/\tau_{\text{ee}}$ increases rapidly with electron temperature; for example, $1/\tau_{\text{ee}} \approx 4/\tau_{\text{eph}}$ already at $T = 600\,\text{K}$, which is still well within the collisionless regime ($\omega_{\text{p}}\tau_{\text{ee}} \approx 13$). We note that graphene encapsulated by hBN has relatively weak electron-electron interaction, due to a larger value of ϵ^*. Therefore one would expect the electron-electron damping mechanism to be the dominant one in graphene deposited on substrates with smaller ϵ^*, e.g., on SiO_2 with $\epsilon^* \approx 2.45$, and, even more so, in freestanding graphene. Finally, we note that recent experiments have demonstrated that plasmons in systems with strong spin-orbit coupling can be observed directly by Raman spectroscopy [34]. Such a situation can be achieved in graphene on transition-metal dichalcogenide substrates. We hope that the results of our paper will be useful for the interpretation of the existing and future experiments.

ACKNOWLEDGMENTS

We are grateful to D. Basov, A. Chubukov, L. Glazman, A. Levchenko, E. Mishchenko, and M. Reizer for stimulating discussions. This work was supported by the U.S. National Science Foundation under Grants No. DMR-1720816 (P.S. and D.L.M.) and No. DMR-2224000 (D.L.M.), by the European Commission under the EU Horizon 2020 MSCA-RISE-2019 program (Project No. 873028 HYDROTRONICS) and the Leverhulme Trust under Grant No. RPG-2019-363 (A.P.), and by the Ministry of Education, Singapore,

under its Research Centre of Excellence award to the Institute for Functional Intelligent Materials (I-FIM, Project No. EDUNC-33-18-279-V12) (G.V.). During the completion of the manuscript, P.S. was supported by MRSEC through Grant No. DMR-2011401. D.L.M. acknowledges the hospitality of the Kavli Institute for Theoretical Physics (KITP), Santa Barbara, supported by the National Science Foundation under Grants No. NSF PHY-1748958 and No. PHY-2309135.

APPENDIX A: PLASMON DAMPING AT FINITE TEMPERATURE WITHIN THE RANDOM-PHASE APPROXIMATION

Within the RPA, the plasmon mode is the solution of the following equation:

$$1 - V_{\mathbf{q}}^{(0)}\Pi(q,\omega) = 0, \tag{A1}$$

where $V_{\mathbf{q}}^{(0)}$ is the bare Coulomb potential and

$$\Pi(q,\omega) = 2\int \frac{d^D k}{(2\pi)^D}\frac{n_{\rm F}(\varepsilon_{\mathbf{k}}) - n_{\rm F}(\varepsilon_{\mathbf{k}+\mathbf{q}})}{\omega - \varepsilon_{\mathbf{k}+\mathbf{q}} + \varepsilon_{\mathbf{k}} + i0^+} \tag{A2}$$

is the polarization bubble (Lindhard function). The plasmon linewidth is determined by the imaginary part of $\Pi(q,\omega)$. For small q,

$$\mathrm{Im}\Pi(q,\omega) = 2\pi\omega\int \frac{d^D k}{(2\pi)^D} n'_{\rm F}(\varepsilon_{\mathbf{k}})\delta(\omega - \mathbf{q}\cdot\mathbf{k}/m). \tag{A3}$$

In two dimensions ($D = 2$) and for a parabolic dispersion with mass m,

$$\begin{aligned}\mathrm{Im}\Pi(q,\omega) &= \omega\int_0^\infty \frac{dk k}{2\pi} n'_{\rm F}(\varepsilon_{\mathbf{k}})\int_0^{2\pi} d\phi\,\delta(\omega - qk\cos\phi/m)\\ &= \frac{m\omega}{\pi q}\int_{m|\omega|/q}^\infty dk\, k\frac{n'_{\rm F}(\varepsilon_{\mathbf{k}})}{\sqrt{k^2 - \left(\frac{m\omega}{q}\right)^2}}.\end{aligned} \tag{A4}$$

Changing the integration variable from k to $\epsilon = k^2/2m$, expressing ϵ in units of $E_{\rm F}$ as $\epsilon = xE_{\rm F}$, and defining $\nu \equiv \omega/qv_{\rm F}$, we obtain

$$-\mathrm{Im}\Pi(q,\omega) = \frac{m\nu}{\pi}\frac{E_{\rm F}}{T}\int_{\nu^2}^\infty \frac{dx}{\sqrt{x-\nu^2}}\frac{1}{4\cosh^2\left[(x-1)\frac{E_{\rm F}}{2T}\right]}. \tag{A5}$$

We are interested in the plasmon range, when $\nu \gg 1$, such that $x \geqslant \nu \gg 1$. In the degenerate case, we also have $E_{\rm F} \gg T$; thus the argument of cosh is always large, and $\cosh z \approx e^z/2$. The integral can be then simplified as

$$\begin{aligned}-\mathrm{Im}\Pi(q,\omega) &\approx \frac{m\nu}{\pi}\frac{E_{\rm F}}{T}e^{E_{\rm F}/T}\int_{\nu^2}^\infty \frac{dx e^{-xE_{\rm F}/T}}{\sqrt{x-\nu^2}}\\ &= \frac{m\nu}{\pi}\sqrt{\frac{E_{\rm F}}{T}}e^{-\frac{E_{\rm F}}{T}(\nu^2-1)}\int_0^\infty \frac{dy e^{-y}}{\sqrt{y}}\\ &= \frac{m\nu}{\sqrt{\pi}}\sqrt{\frac{E_{\rm F}}{T}}e^{-\frac{E_{\rm F}}{T}(\nu^2-1)}\\ &= m\frac{\omega}{v_{\rm F}q}\sqrt{\frac{E_{\rm F}}{\pi T}}e^{-\frac{E_{\rm F}}{T}\left(\frac{\omega^2}{v_{\rm F}^2q^2}-1\right)}.\end{aligned} \tag{A6}$$

(This result was presented in Ref. [10] without a factor of $e^{E_{\rm F}/T}$.)

The plasmon linewidth is given by

$$\Gamma(q) = -\frac{\omega_{\rm p}(q)V_q}{2}\Pi(q,\omega_{\rm p}(q)), \tag{A7}$$

where $\omega_{\rm p}(q) = v_{\rm F}\sqrt{\kappa q/2}$ is the plasmon frequency, $\kappa = 2me^2$ is the inverse Thomas-Fermi screening radius, and $V_{\mathbf{q}}^{(0)} = 2\pi e^2/q$. According to Eq. (53), the inverse quality factor is given by

$$\gamma(q) = \frac{2\Gamma(q)}{\omega_{\rm p}(q)} = \sqrt{\frac{\pi E_{\rm F}}{2T}}\left(\frac{\kappa}{q}\right)^{3/2}e^{-\frac{E_{\rm F}}{T}\left(\frac{\kappa}{2q}-1\right)}, \tag{A8}$$

which is exponentially small for $q \ll \kappa$ and $T \ll E_{\rm F}$.

APPENDIX B: DERIVATION OF EQ. (18)

Substituting $W_{\mathbf{k},\mathbf{p}\to\mathbf{k}'\mathbf{p}'} = 8\pi V^2(|\mathbf{k}-\mathbf{k}'|)$ into Eq. (16), eliminating one of the four momenta in favor of the momentum transfer $\mathbf{Q} = \mathbf{k}' - \mathbf{k} = \mathbf{p} - \mathbf{p}'$, and introducing the energy transfer via $\Omega = \varepsilon_{\mathbf{k}'} - \varepsilon_{\mathbf{k}} = \varepsilon_{\mathbf{p}} - \varepsilon_{\mathbf{p}'}$, we obtain

$$\begin{aligned}\mathrm{Re}\sigma(q,\omega) = \frac{8\pi e^2 q^2 N_{\rm F}^2}{8T\omega^4}\int\frac{d^2Q}{(2\pi)^2}\int d\Omega\int d\varepsilon_{\mathbf{k}}\int d\varepsilon_{\mathbf{p}}\int\frac{d\theta_{\mathbf{pQ}}}{2\pi}\int\frac{d\theta_{\mathbf{kQ}}}{2\pi}V_{\mathbf{Q}}^2 n_{\mathbf{k}}n_{\mathbf{p}}(1-n_{\mathbf{k}+\mathbf{Q}})(1-n_{\mathbf{p}-\mathbf{Q}})\\ \times\delta(\Omega+\varepsilon_{\mathbf{k}}-\varepsilon_{\mathbf{k}+\mathbf{Q}})\delta(\Omega-\varepsilon_{\mathbf{p}}+\varepsilon_{\mathbf{p}-\mathbf{Q}})[\mathbf{v}_{\mathbf{k}}(\mathbf{v}_{\mathbf{k}}\cdot\hat{\mathbf{q}}) + \mathbf{v}_{\mathbf{p}}(\mathbf{v}_{\mathbf{p}}\cdot\hat{\mathbf{q}}) - \mathbf{v}_{\mathbf{k}+\mathbf{Q}}(\mathbf{v}_{\mathbf{k}+\mathbf{Q}}\cdot\hat{\mathbf{q}}) - \mathbf{v}_{\mathbf{p}-\mathbf{Q}}(\mathbf{v}_{\mathbf{p}-\mathbf{Q}}\cdot\hat{\mathbf{q}})]^2,\end{aligned} \tag{B1}$$

where $N_{\rm F} = m/2\pi$ is the density of states and $\theta_{\mathbf{ab}}$ is the angle between the vectors $\mathbf{a}$ and $\mathbf{b}$. Expanding the factor in the square brackets in Eq. (B1) in $Q/k_{\rm F}$ to order Q^2 and projecting the electron momenta onto the Fermi surface, we obtain

$$[\cdots]^2 = \frac{k_{\rm F}^2Q^2}{m^4}(\hat{\mathbf{Q}}\cos\theta_{\mathbf{kq}} + \hat{\mathbf{k}}\cos\theta_{\mathbf{qQ}} - \hat{\mathbf{Q}}\cos\theta_{\mathbf{pq}} - \hat{\mathbf{p}}\cos\theta_{\mathbf{qQ}})^2. \tag{B2}$$

Writing $\theta_{\mathbf{qp}} = \theta_{\mathbf{qQ}} + \theta_{\mathbf{Qp}}$, $\theta_{\mathbf{qk}} = \theta_{\mathbf{qQ}} + \theta_{\mathbf{Qk}}$ and integrating over $\theta_{\mathbf{qQ}}$, we get

$$\int_0^{2\pi}\frac{d\theta_{\mathbf{qQ}}}{2\pi}[\cdots]^2 = 2\frac{k_{\rm F}^2Q^2}{m^4}[3-\cos(\theta_{\mathbf{kQ}}+\theta_{\mathbf{pQ}})]\sin^2\frac{\theta_{\mathbf{kQ}}-\theta_{\mathbf{pQ}}}{2}. \tag{B3}$$

To integrate over $\theta_{\mathbf{kQ}}$ and $\theta_{\mathbf{pQ}}$, we use the constraints imposed by energy conservation via the delta functions in Eq. (B1). With $\Omega = 0$ and $O(Q^2)$ terms discarded, these constraints are $\theta_{\mathbf{kQ}} = \pm\pi/2$ and $\theta_{\mathbf{pQ}} = \pm\pi/2$. The last term in Eq. (B3) ensures

that only the combinations of $\theta_{\mathbf{kQ}} = -\theta_{\mathbf{pQ}} = \pm\pi/2$ give nonzero contributions. Summing up these contributions, we obtain

$$\int_0^{2\pi} d\theta_{\mathbf{kQ}} \int_0^{2\pi} d\theta_{\mathbf{pQ}} [\cdots]^2 = \frac{8k_F^2 Q^2}{m^4}. \tag{B4}$$

Next, the energy integration gives

$$\int d\Omega \int d\varepsilon_{\mathbf{k}} \int d\varepsilon_{\mathbf{p}} [1 - n_F(\varepsilon_{\mathbf{k}} + \Omega)][1 - n_F(\varepsilon_{\mathbf{p}} - \Omega)] n_F(\varepsilon_{\mathbf{p}}) n_F(\varepsilon_{\mathbf{k}}) = \frac{2\pi^2 T^3}{3}. \tag{B5}$$

Substituting Eqs. (B4) and (B5) back into Eq. (B1), and calculating the Q integral to leading logarithmic accuracy with an upper limit cutoff at $Q \sim k_F$, we arrive at the final result,

$$\mathrm{Re}\sigma(q,\omega) = \frac{e^2\kappa^2}{6m^2} \frac{q^2T^2}{\omega^4} \int_0^{k_F} \frac{dQQ}{(Q+\kappa)^2} \approx \frac{e^2\kappa^2}{12m^2} \frac{q^2T^2}{\omega^4} \ln\frac{k_F}{\kappa}, \tag{B6}$$

which is Eq. (18) of the main text.

APPENDIX C: OPTICAL CONDUCTIVITY VIA THE MRG METHOD

1. 2D electron gas

In this Appendix, we derive Eq. (31) of the main text. We start with a 2D version of Eq. (24) with $\mathcal{A}$ given by the sum of the first term in Eq. (29) and the entire equation (30):

$$\mathcal{A} = \frac{V_{\mathbf{Q}}}{m} \left\{ q^2 + 2\frac{(\mathbf{q}\cdot\mathbf{Q})[\mathbf{q}\cdot(\mathbf{p}-\mathbf{k}-\mathbf{Q})]}{m\omega} \right\}, \tag{C1}$$

where $V_Q = 2\pi e^2/(q+\kappa)$ is the screened Coulomb potential. Replacing the integration over $\mathbf{p}$ ($\mathbf{k}$) by that over $\varepsilon_{\mathbf{p}}$ ($\varepsilon_{\mathbf{k}}$) and angles $\theta_{\mathbf{pQ}}$ ($\theta_{\mathbf{kQ}}$), and confining the energy integrations to the narrow vicinity of the Fermi energy, we obtain

$$\begin{aligned}\mathrm{Re}\sigma(q,\omega) = {} & \frac{e^2(1-e^{-\omega/T})}{(2\pi)^3\omega^3q^2} N_F^2 \int d^2Q \int_{-\infty}^{\infty} d\varepsilon_{\mathbf{p}} \int_{-\infty}^{\infty} d\varepsilon_{\mathbf{k}} \int_{-\infty}^{\infty} d\Omega \int_0^{2\pi} d\theta_{\mathbf{pQ}} \int_0^{2\pi} d\theta_{\mathbf{kQ}} \mathcal{A}^2(\theta_{\mathbf{kQ}}, \theta_{\mathbf{pQ}}) n_F(\varepsilon_{\mathbf{p}}) n_F(\varepsilon_{\mathbf{k}}) \\ & \times [1 - n_F(\varepsilon_{\mathbf{k}} - \Omega)][1 - n_F(\varepsilon_{\mathbf{p}} + \Omega + \omega)] \delta(\mathbf{v}_{\mathbf{p}}\cdot\mathbf{Q} - Q^2/2m + (\Omega+\omega)) \delta(\mathbf{v}_{\mathbf{k}}\cdot\mathbf{Q} + Q^2/2m + \Omega),\end{aligned} \tag{C2}$$

where $N_F = m/2\pi$ is the density of states per spin orientation. Writing $\theta_{\mathbf{qp}} = \theta_{\mathbf{qQ}} + \theta_{\mathbf{Qp}}$ and $\theta_{\mathbf{qk}} = \theta_{\mathbf{qQ}} + \theta_{\mathbf{Qk}}$, and folding the angular integrations down to the $(0, \pi)$ intervals, we get

$$\begin{aligned}\mathrm{Re}\sigma(q,\omega) = {} & \frac{e^2(1-e^{-\omega/T})}{(2\pi)^3\omega^3q^2} N_F^2 \int_{-\infty}^{\infty} d\varepsilon_{\mathbf{k}} \int_{-\infty}^{\infty} d\varepsilon_{\mathbf{p}} \int_{-\infty}^{\infty} d\Omega \int d^2Q \int_0^{\pi} d\theta_{\mathbf{pQ}} \int_0^{\pi} d\theta_{\mathbf{kQ}} \\ & \times [\mathcal{A}^2(\theta_{\mathbf{kQ}}, \theta_{\mathbf{pQ}}) + \mathcal{A}^2(-\theta_{\mathbf{kQ}}, -\theta_{\mathbf{pQ}}) + \mathcal{A}^2(-\theta_{\mathbf{kQ}}, \theta_{\mathbf{pQ}}) + \mathcal{A}^2(\theta_{\mathbf{kQ}}, -\theta_{\mathbf{pQ}})] n_F(\varepsilon_{\mathbf{p}}) n_F(\varepsilon_{\mathbf{k}}) (1 - n_F(\varepsilon_{\mathbf{k}} - \Omega)) \\ & \times (1 - n_F(\varepsilon_{\mathbf{p}} + \Omega + \omega)) \delta(\mathbf{v}_{\mathbf{p}}\cdot\mathbf{Q} + Q^2/2m - (\Omega+\omega)) \delta(\mathbf{v}_{\mathbf{k}}\cdot\mathbf{Q} - Q^2/2m - \Omega),\end{aligned} \tag{C3}$$

where

$$\mathcal{A}(\theta_{\mathbf{kQ}}, \theta_{\mathbf{p,Q}}) = \frac{q^2 V_{\mathbf{Q}}}{m} \left\{ 1 - 2\frac{Q\cos\theta_{\mathbf{qQ}}}{m\omega} [k_F \cos(\theta_{\mathbf{qQ}} + \theta_{\mathbf{Qp}}) - k_F \cos(\theta_{\mathbf{qQ}} + \theta_{\mathbf{Qk}}) + Q\cos\theta_{\mathbf{qQ}}] \right\} \tag{C4}$$

is the projection of $\mathcal{A}$ onto the Fermi surface.

To perform the angular integrations in Eq. (C3), we use the constraints imposed by the delta functions in Eq. (C4), i.e.,

$$\begin{aligned}\theta_{\mathbf{kQ}} &= \cos^{-1}\left[\frac{\Omega}{v_F Q} + \frac{Q}{2k_F}\right], \\ \theta_{\mathbf{pQ}} &= \cos^{-1}\left[\frac{(\Omega+\omega)}{v_F Q} - \frac{Q}{2k_F}\right].\end{aligned} \tag{C5}$$

Simple trigonometry yields

$$\begin{aligned}\cos(\theta_{\mathbf{qQ}} \pm \theta_{\mathbf{Qp}}) &= \cos\theta_{\mathbf{qQ}} \left(\frac{\Omega+\omega}{v_F Q} - \frac{Q}{2k_F}\right) \mp \sin\theta_{\mathbf{qQ}} \sqrt{1 - \left(\frac{(\Omega+\omega)}{v_F Q} - \frac{Q}{2k_F}\right)^2}, \\ \cos(\theta_{\mathbf{qQ}} \pm \theta_{\mathbf{Qk}}) &= \cos\theta_{\mathbf{qQ}} \left(\frac{\Omega}{v_k Q} + \frac{Q}{2k_F}\right) \mp \sin\theta_{\mathbf{qQ}} \sqrt{1 - \left(\frac{\Omega}{v_F Q} + \frac{Q}{2k_F}\right)^2}.\end{aligned} \tag{C6}$$

Substituting Eq. (C6) back into Eq. (C4), we get

$$\mathcal{A}(\theta_{\mathbf{kQ}},\theta_{\mathbf{pQ}})=\mathcal{A}(-\theta_{\mathbf{kQ}},-\theta_{\mathbf{pQ}})=\frac{q^2V_{\mathbf{Q}}}{m}\times\left\{1-2\cos^2\theta_{\mathbf{qQ}}-2\frac{k_{\mathrm{F}}Q}{m\omega}\cos\theta_{\mathbf{qQ}}\sin\theta_{\mathbf{qQ}}\left[\sqrt{1-\left(\frac{\Omega+\omega}{v_{\mathrm{F}}Q}-\frac{Q}{2k_{\mathrm{F}}}\right)^2}-\sqrt{1-\left(\frac{\Omega}{v_{\mathrm{F}}Q}+\frac{Q}{2k_{\mathrm{F}}}\right)^2}\right]\right\},\tag{C7a}$$

$$\mathcal{A}(\pm\theta_{\mathbf{kQ}},\mp\theta_{\mathbf{pQ}})=\frac{q^2V_{\mathbf{Q}}}{m}\left\{1-2\cos^2\theta_{\mathbf{qQ}}\mp2\frac{k_{\mathrm{F}}Q}{m\omega}\cos\theta_{\mathbf{qQ}}\sin\theta_{\mathbf{qQ}}\left[\sqrt{1-\left(\frac{\Omega+\omega}{v_{\mathrm{F}}Q}-\frac{Q}{2k_{\mathrm{F}}}\right)^2}+\sqrt{1-\left(\frac{\Omega}{v_{\mathrm{F}}Q}+\frac{Q}{2k_{\mathrm{F}}}\right)^2}\right]\right\}.\tag{C7b}$$

We anticipate (and will prove later) that typical values of the energy and momentum transfers are such that $\Omega\sim\omega\ll v_{\mathrm{F}}Q$ and $Q\ll k_{\mathrm{F}}$. If so, then the factor in square brackets in Eq. (C7a) is small, as

$$\sqrt{1-\left(\frac{\Omega+\omega}{v_{\mathrm{F}}Q}-\frac{Q}{2k_{\mathrm{F}}}\right)^2}-\sqrt{1-\left(\frac{\Omega}{v_{\mathrm{F}}Q}+\frac{Q}{2k_{\mathrm{F}}}\right)^2}\approx-\frac{1}{2}\frac{\omega+2\Omega}{v_{\mathrm{F}}Q}\left(\frac{\omega}{v_{\mathrm{F}}Q}-\frac{Q}{k_{\mathrm{F}}}\right),\tag{C8}$$

and can be neglected. Under the same conditions, the factor in square brackets in Eq. (C7b) is almost equal to 2. With these simplifications, we have

$$\mathcal{A}(\theta_{\mathbf{kQ}},\theta_{\mathbf{pQ}})=\mathcal{A}'(-\theta_{\mathbf{kQ}},-\theta_{\mathbf{pQ}})\approx\frac{q^2V_{\mathbf{Q}}}{m}(1-2\cos^2\theta_{\mathbf{qQ}}),$$
$$\mathcal{A}(\pm\theta_{\mathbf{kQ}},\mp\theta_{\mathbf{pQ}})\approx\frac{q^2V_{\mathbf{Q}}}{m}\left(1-2\cos^2\theta_{\mathbf{qQ}}\mp4\frac{v_{\mathrm{F}}Q}{\omega}\cos\theta_{\mathbf{qQ}}\sin\theta_{\mathbf{qQ}}\right).\tag{C9}$$

The square brackets in Eq. (C3) can now be written as

$$\mathcal{A}^2(\theta_{\mathbf{kQ}},\theta_{\mathbf{pQ}})+\mathcal{A}^2(-\theta_{\mathbf{kQ}},-\theta_{\mathbf{pQ}})+\mathcal{A}^2(-\theta_{\mathbf{kQ}},\theta_{\mathbf{pQ}})+\mathcal{A}^2(\theta_{\mathbf{kQ}},-\theta_{\mathbf{pQ}})$$
$$=\frac{q^4V_{\mathbf{Q}}^2}{m^2}\left[4\left(1-2\cos^2\theta_{\mathbf{qQ}}\right)^2+32\frac{(v_{\mathrm{F}}Q)^2}{\omega^2}\cos^2\theta_{\mathbf{qQ}}\sin^2\theta_{\mathbf{qQ}}\right].\tag{C10}$$

On calculating the angular and energy integrals as $(2\pi)^{-1}\int_0^{2\pi}d\theta_{\mathbf{qQ}}(1-2\cos^2\theta_{\mathbf{qQ}})^2=1/2$ and $(2\pi)^{-1}\int_0^{2\pi}d\theta_{\mathbf{qQ}}\cos^2\theta_{\mathbf{qQ}}\sin^2\theta_{\mathbf{qQ}}=1/8$, and as

$$\int_{-\infty}^{\infty}d\Omega\int_{-\infty}^{\infty}d\varepsilon_{\mathbf{p}}\int_{-\infty}^{\infty}d\varepsilon_{\mathbf{k}}n_{\mathrm{F}}(\varepsilon_{\mathbf{p}})n_{\mathrm{F}}(\varepsilon_{\mathbf{k}})(1-n_{\mathrm{F}}(\varepsilon_{\mathbf{k}}-\Omega))(1-n_{\mathrm{F}}(\varepsilon_{\mathbf{p}}+\Omega+\omega))=\frac{\omega(\omega^2+4\pi^2T^2)}{6(1-e^{-\omega/T})},\tag{C11}$$

respectively, $\mathrm{Re}\sigma$ is reduced to

$$\mathrm{Re}\sigma(q,\omega)=\frac{e^2}{12\pi^2}\frac{q^2N_{\mathrm{F}}^2}{k_{\mathrm{F}}^2}\frac{\omega^2+4\pi^2T^2}{\omega^2}\int\frac{dQ}{Q}V_{\mathbf{Q}}^2\left[1+2\left(\frac{v_{\mathrm{F}}Q}{\omega}\right)^2\right].\tag{C12}$$

With $V_{\mathbf{Q}}$ given by Eq. (3), the integrals over Q in the last equation are calculated to leading logarithm accuracy as

$$\int_{\max\{|\omega|,T\}/v_{\mathrm{F}}}\frac{dQ}{Q}\frac{1}{(Q+\kappa)^2}\approx\frac{1}{\kappa^2}\ln\frac{v_{\mathrm{F}}\kappa}{\max\{|\omega|,T\}},\tag{C13a}$$

$$\int_0^{k_{\mathrm{F}}}\frac{dQQ}{(Q+\kappa)^2}\approx\ln\frac{k_{\mathrm{F}}}{\kappa}.\tag{C13b}$$

Substituting the results of the Q integration back into Eq. (C12) gives Eq. (31) of the main text.

2. 3D electron gas

The starting point for the 3D case is an expression which differs from Eq. (C2) only in the angular integrals:

$$\mathrm{Re}\sigma(q,\omega)=\frac{e^2(1-e^{-\omega/T})}{4(2\pi)^4\omega^3q^2}N_{\mathrm{F}}^2\int_0^{\infty}dQQ^2\int_{-\infty}^{\infty}d\varepsilon_{\mathbf{p}}\int_{-\infty}^{\infty}d\varepsilon_{\mathbf{k}}\int_{-\infty}^{\infty}d\Omega\int d\mathcal{O}_{\mathbf{Qq}}\int d\mathcal{O}_{\mathbf{pQ}}\int d\mathcal{O}_{\mathbf{kQ}}\mathcal{A}^2$$
$$\times n_{\mathrm{F}}(\varepsilon_{\mathbf{p}})n_{\mathrm{F}}(\varepsilon_{\mathbf{k}})[1-n_{\mathrm{F}}(\varepsilon_{\mathbf{k}}-\Omega)][1-n_{\mathrm{F}}(\varepsilon_{\mathbf{p}}+\Omega+\omega)]\delta(\mathbf{v}_{\mathbf{p}}\cdot\mathbf{Q})\delta(\mathbf{v}_{\mathbf{k}}\cdot\mathbf{Q}),\tag{C14}$$

where $d\mathcal{O}_{\mathbf{nn}'}=dx_{\mathbf{nn}'}d\phi_{\mathbf{n}}$, $x_{\mathbf{nn}'}=\cos\theta_{\mathbf{nn}'}$, $\theta'_{\mathbf{nn}}$ is the polar angle of vector $\mathbf{n}$ measured with respect to $\mathbf{n}'$, and $\phi_{\mathbf{n}}$ is the azimuthal angle of $\mathbf{n}$. Please note that, based on the result for the 2D case, we already discarded the subleading terms in the delta functions.

Anticipating that, as in 2D, Eq. (30) gives the leading contribution to the conductivity, we replace $\mathcal{A}$ by $\mathcal{A}_2$ in Eq. (C14). In a spherical system, $\mathcal{A}$ can be written as

$$\mathcal{A} = \mathcal{A}_2 = 2V_{\mathbf{Q}} \frac{q^2 Q x_{\mathbf{Q}}}{m^2 \omega} [k_{\mathrm{F}}(x_{\mathbf{pq}} - x_{\mathbf{kq}}) - Q x_{\mathbf{Qq}}], \tag{C15}$$

where $V_{\mathbf{Q}} = 4\pi e^2/(Q^2 + \kappa^2)$ is the screened Coulomb potential in 3D, $x_{\mathbf{pq}} = x_{\mathbf{pQ}} x_{\mathbf{Qq}} + \sqrt{1 - x_{\mathbf{pQ}}^2}\sqrt{1 - x_{\mathbf{Qq}}^2}\cos(\varphi_{\mathbf{p}} - \phi_{\mathbf{Q}})$, and similarly for $x_{\mathbf{kq}}$. Next, we take into account the constraints imposed by the delta functions in Eq. (C14), i.e., $x_{\mathbf{pQ}} = 0$ and $x_{\mathbf{kQ}} = 0$, and also, using the condition $Q \ll k_{\mathrm{F}}$, neglect the $Q x_{\mathbf{Qq}}$ term in Eq. (C15). Then Eq. (C15) is simplified to

$$\mathcal{A} = 2V_{\mathbf{Q}} \frac{q^2}{m} \frac{v_{\mathrm{F}} Q}{\omega} x_{\mathbf{Qq}} \sqrt{1 - x_{\mathbf{Qq}}^2} [\cos(\phi_p - \phi_Q) - \cos(\phi_k - \phi_Q)]. \tag{C16}$$

Integrating over the angles, we obtain

$$\int d\mathcal{O}_{\mathbf{Qq}} \int d\mathcal{O}_{\mathbf{pQ}} \int d\,\mathcal{O}_{\mathbf{kQ}} \mathcal{A}^2 \delta(\mathbf{v_p} \cdot \mathbf{Q}) \delta(\mathbf{v_k} \cdot \mathbf{Q}) = \frac{96\pi^3}{15} \frac{q^4 V_Q^2}{m^2 \omega^2}. \tag{C17}$$

Using Eq. (C11) for the energy integration, we arrive at

$$\begin{aligned} R\sigma(q, \omega) &= \frac{e^2 q^2}{60\pi v_{\mathrm{F}}^2 m^2 \omega^2} (4\pi e^2)^2 N_{\mathrm{F}}^2 \frac{\omega^2 + 4\pi^2 T^2}{\omega^2} \int_0^\infty \frac{dQ Q^2}{(Q^2 + \kappa^2)^2} \\ &= \frac{e^2 \kappa}{720} \frac{q^2}{k_{\mathrm{F}}^2} \frac{v_{\mathrm{F}}^2 \kappa^2}{\omega^2} \frac{\omega^2 + 4\pi^2 T^2}{\omega^2}, \end{aligned} \tag{C18}$$

which is Eq. (32) of the main text.

3. Doped monolayer graphene

Expanding the graphene dispersion to $O(q^2)$ as

$$\varepsilon_{\mathbf{p+q}} = v_{\mathrm{D}} |\mathbf{p} + \mathbf{q}| - E_{\mathrm{F}} = \varepsilon_{\mathbf{p}} + \mathbf{v_p} \cdot \mathbf{q} + \frac{q^2 v_{\mathrm{D}}}{2p} \sin^2 \theta_{\mathbf{pq}} \tag{C19}$$

with $\mathbf{v_p} = v_{\mathrm{D}} \mathbf{p}/p$, we obtain

$$\frac{1}{\omega - \varepsilon_{\mathbf{p+q}} + \varepsilon_{\mathbf{p}}} = \frac{1}{\omega} \left[1 + \frac{\mathbf{v_p} \cdot \mathbf{q}}{\omega} + \frac{q^2 v_{\mathrm{D}}}{2p} \sin^2 \theta_{\mathbf{pq}} + \left(\frac{\mathbf{q} \cdot \mathbf{v_p}}{\omega} \right)^2 \right], \tag{C20}$$

and similarly for other terms in Eq. (23). Substituting these expansions into Eq. (23), we obtain

$$\begin{aligned} \mathcal{A} = V_{\mathbf{k}-\mathbf{k}'} &\left[\mathbf{v_p} \cdot \mathbf{q} - \mathbf{v}_{\mathbf{p}'} \cdot \mathbf{q} + \frac{q^2 v_{\mathrm{D}}}{2p} \sin^2 \theta_{\mathbf{pq}} + \frac{q^2 v_{\mathrm{D}}}{2p'} \sin^2 \theta_{\mathbf{p'q}} + \frac{(\mathbf{v_p} \cdot \mathbf{q})^2 - (\mathbf{v}_{\mathbf{p}'} \cdot \mathbf{q})^2}{\omega} \right] \\ + V_{\mathbf{p}'-\mathbf{p}} &\left[\mathbf{v_k} \cdot \mathbf{q} - \mathbf{v}_{\mathbf{k}'} \cdot \mathbf{q} + \frac{q^2 v_{\mathrm{D}}}{2k} \sin^2 \theta_{\mathbf{kq}} + \frac{q^2 v_{\mathrm{D}}}{2k'} \sin^2 \theta_{\mathbf{k'q}} + \frac{(\mathbf{v_k} \cdot \mathbf{q})^2 - (\mathbf{v}_{\mathbf{k}'} \cdot \mathbf{q})^2}{\omega} \right]. \end{aligned} \tag{C21}$$

The momentum transfer Q is defined by $\mathbf{p} - \mathbf{p}' = \mathbf{Q}$, and from momentum conservation we have $\mathbf{k}' - \mathbf{k} = \mathbf{Q} + \mathbf{q}$. As for the parabolic case, the difference between $V_{\mathbf{k}-\mathbf{k}'} = V_{\mathbf{Q+q}}$ and $V_{\mathbf{p}-\mathbf{p}'} = V_{\mathbf{Q}}$ can be neglected. Next, we split $\mathcal{A}$ into two parts as $\mathcal{A} = \mathcal{B} + \mathcal{C}$, where

$$\mathcal{B} = V_{\mathbf{Q}} \mathbf{q} \cdot (\mathbf{v_p} + \mathbf{v_k} - \mathbf{v}_{\mathbf{p}'} - \mathbf{v}_{\mathbf{k}'}) = v_{\mathrm{D}} V_{\mathbf{Q}} \mathbf{q} \cdot \left(\frac{\mathbf{p}}{p} + \frac{\mathbf{k}}{k} - \frac{\mathbf{p} - \mathbf{Q}}{|\mathbf{p} - \mathbf{Q}|} - \frac{\mathbf{k} + \mathbf{Q} + \mathbf{q}}{|\mathbf{k} + \mathbf{Q} + \mathbf{q}|} \right). \tag{C22}$$

Expanding $\mathcal{B}$ to $O(q^2)$, we obtain

$$\mathcal{B} = v_{\mathrm{D}} V_{\mathbf{Q}} \left[\frac{\mathbf{q} \cdot \mathbf{p}}{p} + \frac{\mathbf{q} \cdot \mathbf{k}}{k} - \frac{\mathbf{q} \cdot (\mathbf{p} - \mathbf{Q})}{|\mathbf{p} - \mathbf{Q}|} - \frac{\mathbf{q} \cdot (\mathbf{k} + \mathbf{Q})}{|\mathbf{k} + \mathbf{Q}|} - \frac{q^2 \sin^2 \theta_{\mathbf{k+Q,q}}}{|\mathbf{k} + \mathbf{Q}|} \right]. \tag{C23}$$

Note that if we replace the magnitudes of the momenta in the $O(q)$ part of the last equation (the first four terms), the resultant expression would vanish. To obtain a nonzero result for the $O(q)$ part, we need to expand the magnitudes of the momenta near the Fermi surface. Performing such an expansion in the $O(q)$ part and replacing $|\mathbf{k} + \mathbf{Q}|$ by k_{F} in the last, $O(q^2)$, term, we obtain

$$\mathcal{B} = V_{\mathbf{Q}} \left\{ \frac{q}{k_{\mathrm{F}}} \left[(\varepsilon_{\mathbf{p+Q}} - \varepsilon_{\mathbf{p}}) \cos \theta_{\mathbf{qp}} + (\varepsilon_{\mathbf{k-Q}} - \varepsilon_{\mathbf{k}}) \cos \theta_{\mathbf{qk}} + \frac{Q}{k_{\mathrm{F}}} (\varepsilon_{\mathbf{p+Q}} - \varepsilon_{\mathbf{k}-Q}) \right]_1 - \frac{v_{\mathrm{D}} q^2}{k_{\mathrm{F}}} \sin^2 \theta_{\mathbf{k-Q,q}} \right\}. \tag{C24}$$

Finally, we recall that in our case of $Q \ll k_F$ the last term in $[\cdots]_1$ can be neglected, while $\theta_{\mathbf{k}-\mathbf{Q},\mathbf{q}}$ in the last term can be replaced with $\theta_{\mathbf{kq}}$. With these simplifications,

$$\mathcal{B} = V_{\mathbf{Q}}\left\{\frac{q}{k_F}[(\varepsilon_{\mathbf{p}+\mathbf{Q}} - \varepsilon_{\mathbf{p}})\cos\theta_{\mathbf{qp}} + (\varepsilon_{\mathbf{k}-\mathbf{Q}} - \varepsilon_{\mathbf{k}})\cos\theta_{\mathbf{qk}}] - \frac{v_D q^2}{k_F}\sin^2\theta_{\mathbf{kq}}\right\}. \tag{C25}$$

As the remaining part of Eq. (C21), $\mathcal{C}$, is already proportional to q^2, we can neglect q everywhere else in that part. Then,

$$\mathcal{C} = V_{\mathbf{Q}}\left\{\frac{q^2 v_D}{2}\left[\frac{\sin^2\theta_{\mathbf{pq}}}{p} + \frac{\sin^2\theta_{\mathbf{p}-\mathbf{Q},\mathbf{q}}}{|\mathbf{p}-\mathbf{Q}|} + \frac{\sin^2\theta_{\mathbf{kq}}}{k} + \frac{\sin^2\theta_{\mathbf{k}+\mathbf{Q},\mathbf{q}}}{|\mathbf{k}+\mathbf{Q}|}\right]_2 + \frac{1}{\omega}[(\mathbf{v}_{\mathbf{p}}\cdot\mathbf{q})^2 - (\mathbf{v}_{\mathbf{p}-\mathbf{Q}}\cdot\mathbf{q})^2 + (\mathbf{v}_{\mathbf{k}}\cdot\mathbf{q})^2 - (\mathbf{v}_{\mathbf{k}+\mathbf{Q}}\cdot\mathbf{q})^2]_3\right\}. \tag{C26}$$

Under the condition of $Q \ll k_F$, we can safely set $Q = 0$ in the square brackets denoted by $[\cdots]_2$. Also, because $\mathcal{C}$ is already proportional to q^2, momenta p and k can be replaced by k_F. Then $[\cdots]_2$ is reduced to

$$[\cdots]_2 = \frac{2}{k_F}(\sin^2\theta_{\mathbf{pq}} + \sin^2\theta_{\mathbf{pk}}). \tag{C27}$$

The square brackets denoted by $[\cdots]_3$ vanish at $Q = 0$. Expanding to $O(Q)$ and again replacing p and k by k_F, we obtain

$$[\cdots]_3 = \frac{2q^2 {v_D}^2 Q}{k_F}(F_{\mathbf{p}} - F_{\mathbf{k}}), \tag{C28}$$

where

$$F_{\mathbf{n}} = \cos\theta_{\mathbf{nq}}(\cos\theta_{\mathbf{Qq}} - \cos\theta_{\mathbf{nQ}}). \tag{C29}$$

Substituting Eqs. (C27) and (C28) back into Eq. (C26), we obtain

$$\mathcal{C} = \frac{q^2 v_D V_{\mathbf{Q}}}{k_F}\left[\sin^2\theta_{\mathbf{pq}} + \sin^2\theta_{\mathbf{kq}} + 2\frac{v_D Q}{\omega}(F_{\mathbf{p}} - F_{\mathbf{k}})\right]. \tag{C30}$$

Adding up Eqs. (C25) and (C30), we rewrite $\mathcal{A}$ as the sum of the $O(q)$ and $O(q^2)$ parts:

$$\mathcal{A} = \mathcal{A}_1 + \mathcal{A}_2, \tag{C31a}$$

$$\mathcal{A}_1 = \frac{qV_{\mathbf{Q}}}{k_F}[-(\varepsilon_{\mathbf{p}} - \varepsilon_{\mathbf{p}-\mathbf{Q}})\cos\theta_{\mathbf{qp}} + (\varepsilon_{\mathbf{k}} - \varepsilon_{\mathbf{k}+\mathbf{Q}})\cos\theta_{\mathbf{qk}}], \tag{C31b}$$

$$\mathcal{A}_2 = \frac{q^2 v_D V_{\mathbf{Q}}}{k_F}\left[\sin^2\theta_{\mathbf{pq}} + 2\frac{v_D Q}{\omega}(F_{\mathbf{p}} - F_{\mathbf{k}})\right], \tag{C31c}$$

as given by Eq. (34c) of the main text. On substituting $\mathcal{A}^2 = \mathcal{A}_1^2 + \mathcal{A}_2^2 + 2\mathcal{A}_1\mathcal{A}_2$ into Eq. (24) for the conductivity, we see that $\mathcal{A}_1^2$ and $\mathcal{A}_2^2$ give the q-independent and $O(q^2)$ terms, respectively, while the angular integration nullifies the cross term, $2\mathcal{A}_1\mathcal{A}_2$. The q-independent part of $\mathrm{Re}\sigma$ is exactly the same as that calculated in Ref. [9] and thus need not be discussed here. In what follows, we focus on the $O(q^2)$ part.

First, we assume (and will confirm later) that typical momentum transfers satisfy $Q \gg |\omega|/v_D$. Then the first term in the square brackets in Eq. (C31c) can be neglected, and $\mathcal{A}_2$ is reduced to

$$\mathcal{A}_2 = \frac{2q^2 v_D Q}{m^*\omega}V_{\mathbf{Q}}(F_{\mathbf{p}} - F_{\mathbf{k}}), \tag{C32}$$

where $m^* = k_F/v_D$.

Substituting Eq. (C32) into Eq. (24), we obtain

$$\mathrm{Re}\sigma_2(\mathbf{q},\omega) = \frac{4e^2q^2(1-e^{-\omega/T})}{(2\pi)^3\omega^5}N_v^2 N_F^2\frac{v_D^2}{m^{*2}}\int d^2Q Q^2 V_{\mathbf{Q}}^2\int_{-\infty}^{\infty}d\varepsilon_{\mathbf{p}}\int_{-\infty}^{\infty}d\varepsilon_{\mathbf{k}}\int_{-\infty}^{\infty}d\Omega\int_0^{2\pi}d\theta_{\mathbf{pQ}}\int_0^{2\pi}d\theta_{\mathbf{kQ}}n_F(\varepsilon_{\mathbf{p}})n_F(\varepsilon_{\mathbf{k}}) \times [1-n_F(\varepsilon_{\mathbf{k}}-\Omega)][1-n_F(\varepsilon_{\mathbf{p}}+\Omega+\omega)]\int_0^{2\pi}d\theta_{\mathbf{pQ}}\int_0^{2\pi}d\theta_{\mathbf{kQ}}\left(F_{\mathbf{p}}-F_{\mathbf{k}}\right)^2\delta(\mathbf{v}_{\mathbf{p}}\cdot\mathbf{Q})\delta(\mathbf{v}_{\mathbf{k}}\cdot\mathbf{Q}), \tag{C33}$$

where $N_v = 2$ is the valley degeneracy. The two delta functions in the last equation are the energy-conservation delta functions in Eq. (24), in which we neglected frequencies ω and Ω and also expanded the dispersions to order $O(Q)$. As before, these delta

functions impose the constraints $\cos\theta_{\mathbf{pQ}} = \cos\theta_{\mathbf{kQ}} = 0$. Imposing these constraints and integrating over $\theta_{\mathbf{qQ}}$, we get

$$\mathrm{Re}\sigma_2(\mathbf{q},\omega) = \frac{4e^2q^2(1-e^{-\omega/T})}{\omega^5 m^{*2}(2\pi)^2} N_v^2 N_\mathrm{F}^2 \int dQ Q V_Q^2 \times \int_{-\infty}^{\infty} d\varepsilon_{\mathbf{p}} \int_{-\infty}^{\infty} d\varepsilon_{\mathbf{k}} \int_{-\infty}^{\infty} d\Omega n_\mathrm{F}(\varepsilon_{\mathbf{p}}) n_\mathrm{F}(\varepsilon_{\mathbf{k}})[1-n_\mathrm{F}(\varepsilon_{\mathbf{k}}-\Omega)][1-n_\mathrm{F}(\varepsilon_{\mathbf{p}}+\Omega+\omega)]. \tag{C34}$$

The energy integrals in Eq. (C34) give

$$I = (1-e^{-\omega/T}) \int_{-\infty}^{\infty} d\varepsilon_{\mathbf{p}} \int_{-\infty}^{\infty} d\varepsilon_{\mathbf{k}} \int_{-\infty}^{\infty} d\Omega\, n_\mathrm{F}(\varepsilon_{\mathbf{p}}) n_\mathrm{F}(\varepsilon_{\mathbf{k}})[1-n_\mathrm{F}(\varepsilon_{\mathbf{k}}-\Omega)][1-n_\mathrm{F}(\varepsilon_{\mathbf{p}}+\Omega+\omega)] = \frac{\omega}{6}(\omega^2+4\pi^2T^2), \tag{C35}$$

while the integral over Q is already solved in Eq. (C13b). Combining everything together, we obtain

$$\mathrm{Re}\sigma_2(\mathbf{q},\omega) = \frac{e^2}{24\pi^2}\frac{q^2\kappa^2}{m^{*2}\omega^2}\left(1+4\pi^2\frac{T^2}{\omega^2}\right)\ln\frac{k_\mathrm{F}}{\kappa}, \tag{C36}$$

with $\kappa = 8\pi N_\mathrm{F} e^2$ in graphene, which is Eq. (4c) of the main text.

APPENDIX D: DERIVATION OF EQ. (25)

We consider Eq. (24) for the case of an electron gas with parabolic dispersion. In the limit of $v_\mathrm{F}q/\omega \ll 1$, we can neglect $\mathbf{q}$ in the Fermi functions and write $\mathcal{A} = \mathcal{A}_1 + \mathcal{A}_2$, where $\mathcal{A}_1$ and $\mathcal{A}_2$ are given in Eqs. (29) and (30), respectively. On redefining the integration variables as $\mathbf{p} \to \mathbf{p} + \mathbf{Q}/2$, $\mathbf{k} \to \mathbf{k} - \mathbf{Q}/2$ and $\Omega \to \Omega - \omega$, Eq. (24) becomes

$$\mathrm{Re}\sigma(q,\omega) = \frac{e^2(1-e^{-\omega/T})}{(2\pi)^{3D-1}q^2\omega^3} \int d^DQ \int d^Dp \int d^Dk \int d\Omega \left\{\frac{1}{m}[q^2V_\mathbf{Q} + (\mathbf{Q}\cdot\mathbf{q})(\mathbf{q}\cdot\nabla V_\mathbf{Q})] + \frac{2V_\mathbf{Q}}{m^2\omega}(\mathbf{q}\cdot\mathbf{Q})[\mathbf{q}\cdot(\mathbf{p}-\mathbf{k})]\right\}^2 \times n_\mathrm{F}(\varepsilon_{\mathbf{k}-\mathbf{Q}/2}) n_\mathrm{F}(\varepsilon_{\mathbf{p}+\mathbf{Q}/2})[1-n_\mathrm{F}(\varepsilon_{\mathbf{p}-\mathbf{Q}/2})][1-n_\mathrm{F}(\varepsilon_{\mathbf{k}+\mathbf{Q}/2})]\delta(\mathbf{p}\cdot\mathbf{Q}/m - \Omega + \omega)\delta(\Omega - \mathbf{k}\cdot\mathbf{Q}/m). \tag{D1}$$

Here, we used that $\varepsilon_{\mathbf{p}+\mathbf{Q}/2} - \varepsilon_{\mathbf{p}-\mathbf{Q}/2} = \mathbf{p}\cdot\mathbf{Q}/m$ and $\varepsilon_{\mathbf{k}-\mathbf{Q}/2} - \varepsilon_{\mathbf{k}+\mathbf{Q}/2} = -\mathbf{k}\cdot\mathbf{Q}/m$. Next, we rewrite the $\mathbf{q}\cdot(\mathbf{p}-\mathbf{k})$ factor in the curly brackets in Eq. (D1) as

$$\begin{aligned}\mathbf{q}\cdot(\mathbf{p}-\mathbf{k}) &= (\mathbf{q}\cdot\hat{\mathbf{Q}})[\hat{\mathbf{Q}}\cdot(\mathbf{p}-\mathbf{k})] - \mathbf{q}\cdot\{[(\mathbf{p}-\mathbf{k})\times\hat{\mathbf{Q}}]\times\hat{\mathbf{Q}}\} \\ &\to -(\mathbf{q}\cdot\hat{\mathbf{Q}})\frac{m\omega}{Q} - [(\mathbf{p}-\mathbf{k})\times\hat{\mathbf{Q}}]\cdot(\hat{\mathbf{Q}}\cdot\mathbf{q}),\end{aligned} \tag{D2}$$

where $\hat{\mathbf{Q}} = \mathbf{Q}/Q$. At the last step, we used the fact that the delta functions in the last line of Eq. (D1) allow one to replace $\hat{\mathbf{Q}}\cdot\mathbf{p} \to m(\Omega-\omega)/Q$ and $\hat{\mathbf{Q}}\cdot\mathbf{p} \to m\Omega/Q$. Substituting Eq. (D2) back into Eq. (D1), we write the conductivity as the sum $\mathrm{Re}\sigma(q,\omega) = \mathrm{Re}\sigma_a(q,\omega) + \mathrm{Re}\sigma_b(q,\omega)$, where

$$\mathrm{Re}\sigma_a(q,\omega) = \frac{e^2(1-e^{-\omega/T})}{(2\pi)^{3D-1}q^2\omega^3m^2} \int d^DQ \int d^Dp \int d^Dk \int d\Omega\,[q^2V_\mathbf{Q} + (\mathbf{Q}\cdot\mathbf{q})(\mathbf{q}\cdot\nabla V_\mathbf{Q}) - 2V_\mathbf{Q}(\mathbf{q}\cdot\hat{\mathbf{Q}})^2]^2 \times n_\mathrm{F}(\varepsilon_{\mathbf{k}-\mathbf{Q}/2}) n_\mathrm{F}(\varepsilon_{\mathbf{p}+\mathbf{Q}/2})[1-n_\mathrm{F}(\varepsilon_{\mathbf{p}-\mathbf{Q}/2})][1-n_\mathrm{F}(\varepsilon_{\mathbf{k}+\mathbf{Q}/2})]\delta(\mathbf{p}\cdot\mathbf{Q}/m - \Omega + \omega)\delta(\Omega - \mathbf{k}\cdot\mathbf{Q}/m) \tag{D3}$$

and

$$\mathrm{Re}\sigma_b(q,\omega) = \frac{4e^2(1-e^{-\omega/T})}{(2\pi)^{3D-1}q^2\omega^5m^4} \int d^DQ \int d^Dp \int d^Dk \int d\Omega\, V_\mathbf{Q}^2(\mathbf{q}\cdot\mathbf{Q})^2\{[(\mathbf{p}-\mathbf{k})\times\hat{\mathbf{Q}}]\cdot(\hat{\mathbf{Q}}\times\mathbf{q})\}^2 \times n_\mathrm{F}(\varepsilon_{\mathbf{k}-\mathbf{Q}/2}) n_\mathrm{F}(\varepsilon_{\mathbf{p}+\mathbf{Q}/2})[1-n_\mathrm{F}(\varepsilon_{\mathbf{p}-\mathbf{Q}/2})][1-n_\mathrm{F}(\varepsilon_{\mathbf{k}+\mathbf{Q}/2})]\delta(\mathbf{p}\cdot\mathbf{Q}/m - \Omega + \omega)\delta(\Omega - \mathbf{k}\cdot\mathbf{Q}/m). \tag{D4}$$

We have neglected the cross-products of the two terms in Eq. (D2), since they vanish on angular integration for a homogeneous electron gas. Indeed, the delta functions in Eq. (D1) fix the value of the cosine of the angles between $\mathbf{p}$ and $\mathbf{Q}$ and between $\mathbf{k}$ and $\mathbf{Q}$. For the products of the two terms in Eq. (D2), the solutions of the delta functions yield contributions which are equal in magnitude but opposite in sign. This is because the second term in Eq. (D2) depends on the sines of the angles between $\mathbf{p}$ and $\mathbf{Q}$ and between $\mathbf{k}$ and $\mathbf{Q}$.

We first focus on Eq. (D3), which can be further simplified by assuming that $V_\mathbf{Q} \propto (Q^{D-1} + \kappa^{D-1})^{-1}$. Then,

$$\mathrm{Re}\sigma_a(q,\omega) = \frac{(1-e^{-\omega/T})}{(2\pi)^{3D-1}q^2\omega^3m^2} \int d^DQ d^Dp d^Dk d\Omega\, V_\mathbf{Q}^2\left[q^2 - \frac{(D-1)Q^{D-1}}{Q^{D-1}+\kappa^{D-1}}(\hat{\mathbf{Q}}\cdot\mathbf{q})^2 - 2(\mathbf{q}\cdot\hat{\mathbf{Q}})^2\right]^2 n_\mathrm{F}(\varepsilon_{\mathbf{k}-\mathbf{Q}/2}) n_\mathrm{F}(\varepsilon_{\mathbf{p}+\mathbf{Q}/2}) \times [1-n_\mathrm{F}(\varepsilon_{\mathbf{p}-\mathbf{Q}/2})][1-n_\mathrm{F}(\varepsilon_{\mathbf{k}+\mathbf{Q}/2})]\delta(\mathbf{p}\cdot\mathbf{Q}/m - \Omega + \omega)\delta(\Omega - \mathbf{k}\cdot\mathbf{Q}/m). \tag{D5}$$

We note that, using the delta functions, one can rewrite

$$(1-e^{-\omega/T})n_{\rm F}(\varepsilon_{\mathbf{k}-\mathbf{Q}/2})n_{\rm F}(\varepsilon_{\mathbf{p}+\mathbf{Q}/2})[1-n_{\rm F}(\varepsilon_{\mathbf{p}-\mathbf{Q}/2})][1-n_{\rm F}(\varepsilon_{\mathbf{k}+\mathbf{Q}/2})]$$
$$\to [n_B(\Omega)-n_B(\Omega-\omega)][n_{\rm F}(\varepsilon_{\mathbf{k}-\mathbf{Q}/2})-n_{\rm F}(\varepsilon_{\mathbf{k}+\mathbf{Q}/2}][n_{\rm F}(\varepsilon_{\mathbf{p}+\mathbf{Q}/2})-n_{\rm F}(\varepsilon_{\mathbf{p}-\mathbf{Q}/2})], \tag{D6}$$

where $n_B(\omega)=(e^{\omega/T}-1)^{-1}$ is the Bose distribution function. Using this expression and introducing the density-density response function as in Eq. (26), we rewrite Eq. (D5) as

$$\begin{aligned}\mathrm{Re}\sigma_a(q,\omega) &= \frac{1}{2q^2\omega^3m^2}\int\frac{d^DQ}{(2\pi)^D}\int_{-\infty}^{\infty}\frac{d\Omega}{\pi}V_{\mathbf{Q}}^2\left[q^2-\frac{(D-1)Q^{D-1}}{Q^{D-1}+\kappa^{D-1}}(\hat{\mathbf{Q}}\cdot\mathbf{q})^2-2(\mathbf{q}\cdot\hat{\mathbf{Q}})^2\right]^2\\ &\times[n_B(\Omega)-n_B(\Omega-\omega)]\mathrm{Im}\chi_c(Q,\Omega)\mathrm{Im}\chi_c(Q,\Omega-\omega)\\ &= \frac{q^2}{\omega^3m^2}\int_0^{\infty}\frac{d^DQ}{(2\pi)^D}\int_{-\infty}^{\infty}\frac{d\Omega}{\pi}V_{\mathbf{Q}}^2a_D(Q)[n_B(\Omega)-n_B(\Omega-\omega)]Im\chi_c(Q,\Omega)Im\chi_c(Q,\Omega-\omega),\end{aligned} \tag{D7}$$

where

$$\begin{aligned}a_3(Q) &= \frac{23Q^4+18Q^2\kappa^2+7\kappa^4}{30(Q^2+\kappa^2)^2}\xrightarrow{\kappa\to0}\frac{23}{30},\\ a_2(Q) &= \frac{11Q^2+12Q\kappa+4\kappa^2}{16(Q+\kappa)^2}\xrightarrow{\kappa\to0}\frac{11}{16}.\end{aligned} \tag{D8}$$

Note that we are allowed to take the limit of $\kappa\to0$ in $a_D(Q)$ in the limit of weak interaction since the integral in Eq. (D7) remains convergent in this limit.

We now focus on Eq. (D4). Introducing the density-density response function as per Eq. (26) and the current-current response function as

$$\mathrm{Im}\chi_{\alpha\beta}(\mathbf{Q},\nu)\equiv-2\pi\int\frac{d^Dk}{(2\pi)^D}(n_{\rm F}(\varepsilon_{\mathbf{k}+\mathbf{Q}/2})-n_{\rm F}(\varepsilon_{\mathbf{k}-\mathbf{Q}/2})\frac{k_\alpha k_\beta}{m^2}\delta(\mathbf{k}\cdot\mathbf{Q}/m-\nu), \tag{D9}$$

we obtain for Eq. (D4)

$$\begin{aligned}\mathrm{Re}\sigma_b(q,\omega) &= \frac{4e^2}{q^2\omega^5m^2}\int\frac{d^DQ}{(2\pi)^D}\int_{-\infty}^{\infty}\frac{d\Omega}{\pi}V_{\mathbf{Q}}^2(\mathbf{q}\cdot\mathbf{Q})^2\epsilon_{\alpha\beta\gamma}\epsilon_{\alpha'\beta'\gamma'}\hat{\mathbf{Q}}_\beta\hat{\mathbf{Q}}_{\beta'}(\hat{\mathbf{Q}}\times\mathbf{q})_\gamma(\hat{\mathbf{Q}}\times\mathbf{q})_{\gamma'}\\ &\times[n_{\rm B}(\Omega)-n_{\rm B}(\Omega-\omega)]\mathrm{Im}\chi_{\alpha\alpha'}(\boldsymbol{Q},\Omega-\omega)\mathrm{Im}\chi_c(Q,\Omega),\end{aligned} \tag{D10}$$

where $\epsilon_{\alpha\beta\gamma}$ is the Levi-Civita tensor and a sum over repeated Greek indices is implied. Owing to the isotropy of the electron gas, the current-current response function can be written as

$$\chi_{\alpha\beta}(\mathbf{Q},\nu)=\frac{Q_\alpha Q_\beta}{Q^2}\chi_L(Q,\nu)+\left(\delta_{\alpha\beta}-\frac{Q_\alpha Q_\beta}{Q^2}\right)\chi_T(Q,\nu), \tag{D11}$$

where $\chi_L(Q,\nu)$ and $\chi_T(Q,\nu)$ are the longitudinal and transverse current-current response functions, respectively. The imaginary part of the latter is given in Eq. (27), while the former is connected to $\chi_c(Q,\nu)$ by the relation $\nu^2\chi_c(Q,\nu)=Q^2\chi_L(Q,\nu)$. Note that both χ_L and χ_T depend only on the magnitude of $\mathbf{Q}$, a fact that reflects the isotropy and rotational invariance of the electron gas. It can be readily seen that only the term proportional to the Kronecker delta in Eq. (D11) contributes to Eq. (D10), which thus becomes

$$\mathrm{Re}\sigma_b(q,\omega)=\frac{4e^2}{q^2\omega^5m^2}\int\frac{d^DQ}{(2\pi)^D}\int_{-\infty}^{\infty}\frac{d\Omega}{\pi}V_{\mathbf{Q}}^2(\mathbf{q}\cdot\mathbf{Q})^2|\hat{\mathbf{Q}}\times\mathbf{q}|^2[n_{\rm B}(\Omega)-n_{\rm B}(\Omega-\omega)]\mathrm{Im}\chi_T(Q,\Omega-\omega)\mathrm{Im}\chi_c(Q,\Omega). \tag{D12}$$

Finally, performing the angular integration, we get

$$\mathrm{Re}\sigma_b(q,\omega)=b_D\frac{e^2q^2}{\omega^3m^2}\int\frac{d^DQ}{(2\pi)^D}\int_{-\infty}^{\infty}\frac{d\Omega}{\pi}\frac{Q^2}{\omega^2}V_{\mathbf{Q}}^2[n_{\rm B}(\Omega)-n_{\rm B}(\Omega-\omega)]\mathrm{Im}\chi_T(Q,\Omega-\omega)\mathrm{Im}\chi_c(Q,\Omega), \tag{D13}$$

where $b_D=8/15$ for $D=3$ and $b_D=1/2$ for $D=2$. We note that the results given in Eqs. (D7) and (D13) agree with those of Ref. [35] once the conductivity is converted into the dynamical exchange-correlation potential $f_{\rm xc}$ as [17,35]

$$\mathrm{Im}\,f_{\rm xc}(\omega)=\lim_{q\to0}\frac{m^2\omega^3}{n^2e^2q^2}\mathrm{Re}\sigma(q,\omega), \tag{D14}$$

where n is the carrier number density.

[1] F. Roth, A. König, J. Fink, B. Büchner, and M. Knupfer, J. Electron Spectrosc. Relat. Phenom. **195**, 85 (2014).

[2] A. Woessner, M. B. Lundeberg, Y. Gao, A. Principi, P. Alonso-González, M. Carrega, K. Watanabe, T. Taniguchi, G. Vignale, M. Polini, J. Hone, R. Hillenbrand, and F. H. L. Koppens, Nat. Mater. **14**, 421 (2015).

[3] G. X. Ni, L. Wang, M. D. Goldflam, M. Wagner, Z. Fei, A. S. McLeod, M. K. Liu, F. Keilmann, B. Özyilmaz, A. H. Castro Neto, J. Hone, M. M. Fogler, and D. N. Basov, Nat. Photonics **10**, 244 (2016).

[4] D. N. Basov, R. D. Averitt, and D. Hsieh, Nat. Mater. **16**, 1077 (2017).

[5] S. Vig, A. Kogar, M. Mitrano, A. A. Husain, V. Mishra, M. S. Rak, L. Venema, P. D. Johnson, G. D. Gu, E. Fradkin, M. R. Norman, and P. Abbamonte, SciPost Phys. **3**, 026 (2017); M. Mitrano, A. A. Husain, S. Vig, A. Kogar, M. S. Rak, S. I. Rubeck, J. Schmalian, B. Uchoa, J. Schneeloch, R. Zhong, G. D. Gu, and P. Abbamonte, Proc. Natl. Acad. Sci. USA **115**, 5392 (2018); S. J. Thornton, D. B. Liarte, P. Abbamonte, J. P. Sethna, and D. Chowdhury, Nat. Commun. **14**, 3919 (2023); J. Chen, X. Guo, C. Boyd, S. Bettler, C. Kengle, D. Chaudhuri, F. Marashi, A. Husain, J. Schneeloch, G. Gu, P. Phillips, B. Uchoa, T.-C. Chiang, and P. Abbamonte, arXiv:2306.03681.

[6] At finite temperature, particle-hole pairs "leak out" through the continuum boundary, but the spectral weight of the leakage, given by the imaginary part of the charge susceptibility, is exponentially small: $\mathrm{Im}\chi_c(q,\omega) \propto \exp[-(m\omega^2/q^2 - E_\mathrm{F})/2T]$,where m is the electron mass and E_F is the Fermi energy (see Appendix A). Consequently, the plasmon lifetime within RPA is finite but exponentially long.

[7] D. F. DuBois and M. G. Kivelson, Phys. Rev. **186**, 409 (1969).

[8] A. Principi, G. Vignale, M. Carrega, and M. Polini, Phys. Rev. B **88**, 195405 (2013).

[9] P. Sharma, A. Principi, and D. L. Maslov, Phys. Rev. B **104**, 045142 (2021).

[10] E. G. Mishchenko, M. Y. Reizer, and L. I. Glazman, Phys. Rev. B **69**, 195302 (2004).

[11] M. Y. Reizer and V. M. Vinokur, Phys. Rev. B **62**, R16306(R) (2000).

[12] U. Briskot, M. Schütt, I. V. Gornyi, M. Titov, B. N. Narozhny, and A. D. Mirlin, Phys. Rev. B **92**, 115426 (2015).

[13] B. N. Narozhny, I. V. Gornyi, A. D. Mirlin, and J. Schmalian, Ann. Phys. (Berlin) **529**, 1700043 (2017).

[14] A. Lucas and S. Das Sarma, Phys. Rev. B **97**, 115449 (2018).

[15] G. Paasch, Phys. Status Solidi (b) **38**, A123 (1970); P. C. Gibbons and S. E. Schnatterly, Phys. Rev. B **15**, 2420 (1977).

[16] D. Pines and P. Nozières, *The Theory of Quantum Liquids. Volume I: Normal Fermi Liquids* (Benjamin, New York, 1966).

[17] G. Giuliani and G. Vignale, *Quantum Theory of the Electron Liquid* (Cambridge University Press, Cambridge, 2005).

[18] Reference [11] did not account for all relevant diagrams, which led to a violation of gauge invariance, and will not be discussed further.

[19] The earlier form of Eq. (4c), derived in Ref. [8], did not capture the logarithmic factor and also had a different dependence on the coupling constant. In addition, Ref. [8] considered only the $T = 0$ case.

[20] R. N. Gurzhi, J. Expt. Theor. Phys. (U.S.S.R.) **35**, 965 (1958) [Sov. Phys. JETP **35**, 673 (1959)].

[21] Equations (4a)–(4c) are valid in the isotropic approximation, which neglects trigonal warping of the Fermi surfaces. If trigonal warping is taken into account, there is another contribution to the conductivity, which is of a regular FL type. This contribution will be discussed in Sec. V C.

[22] A. A. Abrikosov, *Fundamentals of the Theory of Metals* (North-Holland, Amsterdam, 1988).

[23] V. F. Gantmakher and Y. B. Levinson, *Carrier Scattering in Metals and Semiconductors* (North-Holland, Amsterdam, 1987).

[24] H. K. Pal, V. I. Yudson, and D. L. Maslov, Lith. J. Phys. **52**, 142 (2012).

[25] A. V. Chubukov and D. L. Maslov, Phys. Rev. B **86**, 155136 (2012).

[26] D. L. Maslov and A. V. Chubukov, Phys. Rev. B **86**, 155137 (2012).

[27] D. L. Maslov and A. V. Chubukov, Rep. Prog. Phys. **80**, 026503 (2017).

[28] To make the analysis applicable to an arbitrary electronic dispersion, we defined $\mathcal{A}$ and $\mathcal{A}_\mathrm{ex}$ without a factor of $1/m$, compared with the original notations of MRG [10].

[29] As shown in Ref. [30], the interaction between electrons in the upper and lower Dirac cones gives a subleading (in the leading-logarithm sense) contribution to the optical conductivity.

[30] A. P. Goyal, P. Sharma, and D. L. Maslov, Ann. Phys. (Amsterdam) **456**, 169355 (2023).

[31] S. Conti and G. Vignale, Phys. Rev. B **60**, 7966 (1999).

[32] I. V. Tokatly, Phys. Rev. B **71**, 165105 (2005).

[33] A. Principi, M. Carrega, M. B. Lundeberg, A. Woessner, F. H. L. Koppens, G. Vignale, and M. Polini, Phys. Rev. B **90**, 165408 (2014).

[34] S. Sarkar, A. Lee, G. Blumberg, and S. Maiti, arXiv:2306.11240.

[35] R. Nifosì, S. Conti, and M. P. Tosi, Phys. Rev. B **58**, 12758 (1998).